RESEARCH PAPER

Involvement of 3′,5′-cyclic inosine monophosphate in cystathionine γ-lyase-dependent regulation of the vascular tone

Emma Mitidieri[1] | Valentina Vellecco[1] | Vincenzo Brancaleone[2] |
Domenico Vanacore[1] | Onorina L. Manzo[1] | Emil Martin[3] | Iraida Sharina[3] |
Yekaterina Krutsenko[4] | Maria Chiara Monti[5] | Elva Morretta[5] |
Andreas Papapetropoulos[6,7] | Giuseppe Caliendo[1] | Francesco Frecentese[1] |
Giuseppe Cirino[1] | Raffaella Sorrentino[8] | Roberta d'Emmanuele di Villa Bianca[1] |
Mariarosaria Bucci[1]

[1]Department of Pharmacy, School of Medicine and Surgery, University of Naples Federico II, Naples, Italy

[2]Department of Science, University of Basilicata, Potenza, Italy

[3]McGovern Medical School, Department of Internal Medicine, Division of Cardiology, University of Texas Health Science Center, Houston, Texas, USA

[4]School of Science and Technology, Nazarbayev University, Astana, Kazakhstan

[5]Department of Pharmacy, University of Salerno, Fisciano, SA, Italy

[6]Laboratory of Pharmacology, Department of Pharmacy, National and Kapodistrian University of Athens, Athens, Greece

[7]Clinical, Experimental Surgery and Translational Research Center, Biomedical Research Foundation of the Academy of Athens, Athens, Greece

[8]Department of Molecular Medicine and Medical Biotechnology, School of Medicine and Surgery, University of Naples Federico II, Naples, Italy

Background and Purpose: L-cysteine or hydrogen sulfide (H_2S) donors induce a biphasic effect on precontracted isolated vessels. The contractile effect occurs within a concentration range of 10 nM to 3 μM followed by vasodilatation at 30–100 μM. Here, we have investigated the signalling involved in the H_2S-induced contraction.

Experimental Approach: Vascular response to NaHS or L-cysteine is evaluated on isolated precontracted with phenylephrine vessel rings harvested from wild type, cystathionine γ-lyase ($CSE^{-/-}$), soluble guanylyl cyclase ($sGC_{\alpha 1}^{-/-}$) and endothelial nitric oxide synthase ($eNOS^{-/-}$) knock-out mice. The cAMP, cGMP and inosine 3′,5′-cyclic monophosphate (cIMP) levels are simultaneously quantified using ultra-performance liquid chromatography–tandem mass spectrometry (UPLC-MS/MS) analysis. The involvement of sGC, phosphodiesterase (PDE) 4A and PDE5 are also evaluated.

Key Results: CSE-derived H_2S-induced contraction requires an intact eNOS/NO/sGC pathway and involves cIMP as a second messenger. H_2S contractile effect involves a transient increase of cGMP and cAMP metabolism caused by PDE5 and PDE4A, thus unmasking cIMP contracting action. The stable cell-permeable analogue of cIMP elicits concentration-dependent contraction on a stable background tone induced by phenylephrine. The lack of cIMP, coupled to the hypocontractility

Correspondence
Prof. Giuseppe Cirino, Department of
Pharmacy, School of Medicine and Surgery,
University of Naples Federico II, via
D. Montesano 49, 80131 Naples, Italy.
Email: cirino@unina.it

displayed by vessels harvested from $CSE^{-/-}$ mice, confirms that H$_2$S-induced contraction involves cIMP.

Conclusion and Implications: The endothelium dynamically regulates vessel homeostasis by modulating contractile tone. This also involves CSE-derived H$_2$S that is mediated by cIMP.

KEYWORDS
cyclic nucleotides, cystathionine γ-lyase, gasotransmitters, inosine 3′,5′-cyclic monophosphate, phosphodiesterases, vascular homeostasis, vasoconstriction

1 | INTRODUCTION

It is well established that within the vasculature, **hydrogen sulfide (H$_2$S)** acts as a vasodilating endogenous mediator (Cirino et al., 2017). Several molecular targets have been identified such as potassium channels (i.e. ATP-dependent, calcium-dependent and voltage gated dependent) (Yu et al., 2018; Zhao et al., 2001; Zuidema et al., 2010), **transient receptor potential (TRP)** and chloride and sodium channels (Yu et al., 2018), **phosphodiesterases (PDEs)** (Bucci et al., 2010; Coletta et al., 2012) and **phospholipase A2** (d'Emmanuele di Villa Bianca et al., 2011; d'Emmanuele di Villa Bianca et al., 2010). H$_2$S is endogenously generated by three constitutive enzymes:- **cystathionine γ-lyase (CSE)** and cystathionine β-synthase (CBS), that both use L-cysteine as substrate and require **pyridoxal 5′-phosphate (PLP)** as a co-factor. The third pathway requires two enzymes that operate in tandem:- the PLP-dependent cysteine aspartate aminotransferase (CAT) and 3-mercaptopyruvate sulfurtransferase (MST). All enzymes are expressed in both endothelium and smooth muscle component, and CSE is the most abundant within the vasculature (Cirino et al., 2017). The literature regarding the H$_2$S vasodilatory action is wide; in fact, several studies are showing that *in vitro* H$_2$S relaxes isolated precontracted vessels within the range of 30 μM to 1 mM. Nevertheless, it is known that H$_2$S displays a biphasic effect of H$_2$S, that is, contraction followed by vasodilation on precontracted vessels (d'Emmanuele di Villa Bianca et al., 2011; Kubo et al., 2007; Liu et al., 2011; Webb et al., 2008). Indeed, by themselves L-cysteine and H$_2$S donors do not cause contraction, it is only when isolated vessels are precontracted with phenylephrine with low concentrations of H$_2$S, within a range of 10 nM to 3 μM, induces a further contraction. This increase in contraction over phenylephrine tone induced by H$_2$S requires the presence of the endothelium since its removal prevents this effect. Here, we have investigated the molecular mechanisms leading to the increase in contraction driven by either H$_2$S donors or the substrate L-cysteine. The study has been performed by applying a pharmacological modulation with selective inhibitors, as well as by using genetically modified mice, that is, $CSE^{-/-}$, soluble **guanylyl cyclase (sGC)$_{\alpha1}$**$^{-/-}$ and **eNOS**$^{-/-}$. *In vitro* studies have been also performed to define the role of sGC and of the cyclic nucleotides, namely, cAMP, cGMP and 3′,5′-cyclic inosine monophosphate (cIMP), by simultaneously dosing their levels in mouse aorta by using

What is already known?

- H$_2$S induces a biphasic response in isolated precontracted aorta, that is contraction followed by vasodilation.

What does this study add?

- The obligatory role of endothelium in H$_2$S-induced contraction involves cIMP.

What is the clinical significance?

- H$_2$S signalling through cIMP contributes to vascular homeostasis.

ultra-performance liquid chromatography–tandem mass spectrometry (UPLC-MS/MS) analysis.

2 | METHODS

2.1 | Animals

Animal care and experimental procedures in this study follow specific guidelines of the Italian and the European Council law for experiments involving animals. All procedures were approved by the local animal care office (Centro Servizi Veterinari, Università degli Studi di Napoli, Federico II) and carried out following recommendations for experimental design and analysis in pharmacology care (Ministero della Salute, n. 24/2016 and n. 718/2016). Animal studies were reported in compliance with the ARRIVE guidelines (Percie du Sert et al., 2020) and with the recommendations made by the British Journal of Pharmacology (Kilkenny et al., 2010; Lilley et al., 2020). All procedures

were performed on male C57BL/6J mice (Charles River, Lecco, Italy, RRID:IMSR_CRL:27), male CSE-ablated mice (CSE$^{-/-}$) and wild type littermates on C57BL/6J × 129SvEv (WT), male sGC$_{\alpha1}$ ablated mice (sGC$_{\alpha1}$$^{-/-}$), male endothelial nitric oxide synthase (eNOS)-ablated mice (eNOS$^{-/-}$) and their wild type littermates on C57BL/6J (WT). All animals were older than 20 weeks of age and their weight was within the range of 30–40 g. Animals were kept at temperatures of 23 ± 2°C, humidity range 40%–70% and 12-h light/dark cycles in pathogen-free cages (four mice per cage) with free access to dry feed and water. CSE$^{-/-}$ and their WT (C57BL/6J × 129SvEv) mice are not commercially available and were kindly gifted by Prof. Rui Wang, York University, Toronto, Canada, and bred in our facility. eNOS$^{-/-}$ and sGC$_{\alpha1}$$^{-/-}$ were a kind gift by Prof. Peter Brouckaert, University of Ghent, Belgium.

2.2 | Tissue preparation

Mice were anaesthetized with enflurane (5%) and then killed in CO_2 chamber (70%). The second method applied is exsanguination. The thoracic aorta or carotid artery was rapidly harvested and adherent connective and fat tissue were removed. Tissue was placed in a dish containing Krebs' solution (NaCl 118 mM, KCl 4.7 mM, MgCl$_2$ 1.2 mM, KH$_2$PO$_4$ 1.2 mM, CaCl$_2$ 2.5 mM, NaHCO$_3$ 25 mM and glucose 10.1 mM) and kept at 37°C (Vellecco et al., 2016). In another set of experiments, the aorta was incubated with NaHS 1 μM or vehicle for 5 and 15 min and then used for western blot analysis or cyclic nucleotide determination.

2.3 | Isolated organ bath

2.3.1 | In vitro study on aorta

Five rings of 1–1.5 mm length were cut from each aorta, placed in organ baths (3.0 ml) filled with oxygenated (95% O$_2$–5% CO$_2$) Krebs' solution. The rings were connected to an isometric transducer (Fort 25, World Precision Instruments, 2Biological Instruments, Varese, Italy) associated to PowerLab 8/35 (World Precision Instruments, Biological Instruments, Varese, Italy). The optimal resting tension applied has been previously determined for each mouse strain. The rings were initially stretched until a resting tension of 1.5 g and then were allowed to equilibrate for at least 30 min. During this period, when necessary, the tension was adjusted to 1.5 g, and the bath solution was periodically changed (Brancaleone et al., 2015; Mitidieri et al., 2018). In each set of experiments, rings were firstly challenged with phenylephrine (1 μM) until the responses were reproducible. To verify the integrity of the endothelium, cumulative concentration–response curves to ACh (10 nM to 30 μM) were performed in phenylephrine-precontracted rings. Rings not reaching a relaxation response of at least 75% were discarded (Mitidieri et al., 2018; Severino et al., 2018). Tissues were then

washed and again contracted with phenylephrine (1 μM). Once the plateau was reached, cumulative concentration–response curves to L-cysteine (10 nM to 3 μM) or sodium hydrogen sulfide (NaHS, 10 nM to 3 μM) were performed in the presence or absence of functional endothelium. In another set of experiments, the effect of NaHS on phenylephrine-precontracted rings was evaluated in the presence of L-NIO and ODQ, (eNOS) and sGC inhibitors, respectively. NaHS concentration–response curve was performed on the stable background tone induced by phenylephrine, following 20 min of exposure with inhibitors (10 μM). Next, to evaluate the role of endothelin 1 (ET-1), L-cysteine or NaHS (10 nM to 3 μM) concentration–response curves were performed on the stable background tone induced by phenylephrine (1 μM) in rings incubated for 20 min with FR 139317 (1 nM, a selective ET$_A$ receptor antagonist) or BQ788 (10 μM, a selective ET$_B$ receptor antagonists). In another set of experiments, the contractile response of aortic rings harvested from CSE$^{-/-}$ mice were evaluated following administration of 5-HT (1 nM to 3 μM), the thromboxane analogue, U46619 (1–300 nM) and potassium chloride (KCl, 10–60 mM).

In a separate set of experiments, the concentration–response curve of the cIMP stable analogue, that is, cIMP butyrate (0.1 nM to 1 μM), was performed either on basal tone or phenylephrine-precontracted aortic rings of WT mice.

2.3.2 | In vitro study on carotid arteries

Carotid rings of ~1.0 mm length were cut from each carotid artery, placed in organ baths (3.0 ml) filled with oxygenated (95% O$_2$–5% CO$_2$) Krebs' solution. The rings were mounted on two stainless steel wires (mice: 25-μm diameter) in an organ bath of a small vessel wire myograph (DMT, Aarhus, Denmark) associated with PowerLab 8/35 (World Precision Instruments, Biological Instruments, Varese, Italy). The two wires were connected to a force transducer and a micrometer, respectively, allowing continuous measurement of isometric force development. The rings were initially stretched until a resting tension of 1.5 g was reached and then were allowed to equilibrate for at least 30 min; during this period, the tension was adjusted, when necessary, to 1.5 g and the bath solution was periodically changed. In each set of experiments, rings were first challenged with phenylephrine, 1 μM until the responses were reproducible. To verify the integrity of the endothelium, cumulative concentration–response curves to ACh (10 nM to 30 μM) were performed in phenylephrine-precontracted rings. Rings not reaching a relaxation response of at least 75% were discarded. Tissues were then washed and again contracted with phenylephrine (1 μM) and once the plateau was reached, cumulative concentration–response curves to L-cysteine (10 nM to 300 μM) or NaHS (10 nM to 300 μM) were performed. In another set of experiments, the contractile response of carotid rings harvested from CSE$^{-/-}$ mice was evaluated following administration of phenylephrine (1 nM to 3 μM), 5-HT (1 nM to 3 μM) and thromboxane analogue, U46619 (1–300 nM).

2.4 | Western blot analysis

Tissues were homogenized in modified RIPA buffer (50-mM Tris-HCl pH 8.0, 150-mM NaCl, 0.5% sodium deoxycholate, 0.1% sodium dodecyl sulfate, 1-mM EDTA, 1% Igepal) containing protease inhibitors cocktail. Protein concentration was determined by Bradford assay using BSA as standard. Denatured proteins (70 μg) were separated on 8% sodium dodecyl sulfate-polyacrylamide gels and transferred to a polyvinylidene fluoride membrane. The membranes were blocked by incubation in phosphate buffered saline (PBS) containing 0.1% v/v Tween 20 and 3% nonfat dried milk (Applichem) for 1 h at room temperature and then incubated overnight at 4°C with rabbit polyclonal anti-p-**PDE4A** (1:500; PPD4-140AP) or rabbit polyclonal anti-p-**PDE5** (1:500; PPD5-140AP). The same membranes were stripped and then incubated with rabbit polyclonal anti-PDE4A (1:1000, 16226-1-AP) and rabbit polyclonal anti-PDE5 (1:1000, SC-32884), respectively. Membranes were extensively washed in PBS containing 0.1% v/v Tween 20 before incubation with horseradish peroxidase-conjugated secondary antibody for 2 h at room temperature. Following incubation, membranes were washed and developed using ImageQuant-400 (GE Healthcare, USA). The target protein band intensity was normalized over the intensity of the housekeeping protein β-actin (1:5000, A4700—Clone: AC40). In another set of experiments, the aorta was harvested from $CSE^{-/-}$ mice or WT and 40 μg of protein were separated on 10% sodium dodecyl sulfate-polyacrylamide gels and transferred to a polyvinylidene fluoride membrane. The membranes were incubated overnight at 4°C with mouse monoclonal anti-eNOS (1:1000; 610297). All immuno-related procedures involved comply with the editorial on immunoblotting and immuno-histochemistry (Alexander et al., 2018).

2.5 | Cyclic nucleotide determination

### 2.5.1 | Nucleotide cyclic monophosphate (cNMP) extraction from aorta

The frozen tissues (around 30–40 mg) from three individual animals were pooled (because a large quantity of tissue is needed for the measurements), lyophilized, homogenized in 100% methanol and centrifuged (12,000 rpm, 20 min, 4°C). The supernatant was dried and dissolved in an opportune volume of water 10-mM ammonium acetate and 0.1% acetic acid.

2.5.2 | Calibration curves

Stock solutions of cAMP, cIMP and cGMP (Sigma-Aldrich, Italy) were freshly prepared at 10 μg·μ^{-1} in water. Calibration curves were prepared by mixing the components at final concentrations from 10 pg μl^{-1} to 1 ng μl^{-1} in water 10-mM ammonium acetate and 0.1% acetic acid. The concentration range for the calibration curve was chosen because it encompasses the typical concentrations of nucleotide cyclic monophosphates within the experimental samples.

2.5.3 | UPLC-MS/MS analysis

For liquid chromatography–tandem mass spectrometry (LC-MS/MS) analysis, the chromatographic separation was carried out on the UPLC-MS system Q-TRAP 6500 LC-MS/MS System from AB Sciex equipped with Shimadzu LC-20A LC and AutoSampler system. The mixture was separated on Kinetex C18 from
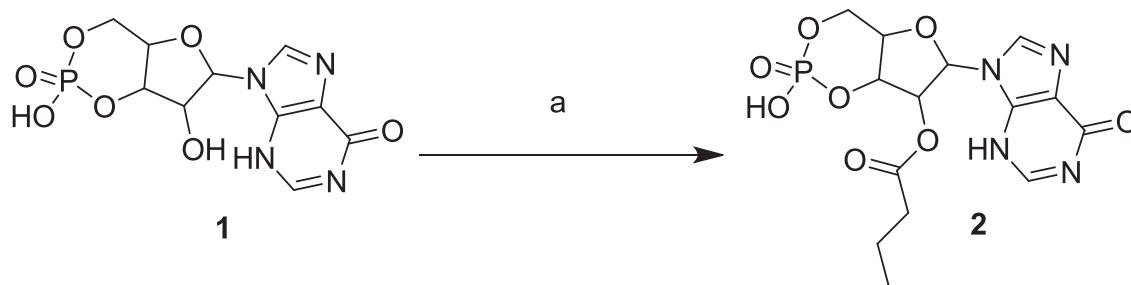

SCHEME 1 Reagents and conditions: Butyric anhydride, triethylamine, anhydrous pyridine, rt, 48 h. all reactions were followed by TLC carried out on Merk silica gel 60 F254 plates with a fluorescent indicator on the plates were visualized with UV light (254 nm). Preparative chromatographic purifications were performed using a silica gel column (Kieselgel 60). Solutions were concentrated with a Buchi R-114 rotary evaporator at low pressure. Melting points, determined using a Buchi melting point B-540 instrument, are uncorrected and represent values obtained on chromatographically purified material. RP-HPLC preparative purification was performed on a Shimadzu prominence LC-20 AP system equipped with a multiwavelength prominence SPD-20A UV–vis detector on a Phenomenex Kinetex XB-C18 column (5 mm, 21.2 × 250 mm) employing the following solvents: A: 100% acetonitrile in 0.1% TFA, B: 100% H_2O in 0.1% TFA. The operational conditions were as follows: Linear-gradient of 5%–70% acetonitrile + 0.1% TFA in 30 min, using a flow rate of 30 ml·min^{-1}. The purity of the products was assessed by analytical RP-HPLC using a Phenomenex Kinetex XB-C18 column (5 μm, 4.6 × 250 mm). The column was connected to a Rheodyne model 7725 injector, a Shimadzu-10 ADsp HPLC system, a Shimadzu SPD-20 a/SPD-20 AV UV–vis detector set to 254 nm. Mass spectra were performed on LTQ Orbitrap XL™ Fourier transform mass spectrometer (FTMS) equipped with an ESI ION MAX™ source (Thermo fisher, San José, USA)—Negative mode. ^{1}H-NMR spectrum was recorded on Varian mercury plus 400 MHz instrument. Chemical shifts are reported in parts per million. The following abbreviations are used to describe peak patterns when appropriate: S (singlet), d (doublet), t (triplet), m (multiplet), bs (broad singlet)

Phenomenex (2.6 μm, 100 Å, LC Column 50 × 2.1 mm). Buffer A contained 10-mM ammonium acetate and 0.1% acetic acid in water and buffer B contained 10-mM ammonium acetate and 0.1% acetic acid in methanol. The optimized UPLC protocol for separating cyclic nucleotide monophosphates (cNMPs) is as follows: 0–0.5 min, 3% B; 0.5–5 min, 3%–8% B; 5–5.1 min, 8%–80% B; 5.1–6 min, 80% B; 6–6.1 min, 80%–3% B; 6.1–10 min, 3% B with a flow rate of 0.4 ml·min⁻¹. Three independent LC-MS/MS runs were performed for each sample. For quantification of the cyclic nucleotide, mass detection was performed on a Qtrap 6500 mass spectrometer (AB Sciex, Foster City, CA) using multiple selected ion monitoring analysis in positive ionization mode. The multiple selected ion monitoring transitions were detected with a 50-ms dwell time. Ion source settings and collision gas pressure were optimized manually (current gas 40 psi, nebulizing gas [pressure] of 30 psi, drying gas [pressure] of 30 psi, ionspray [voltage] of 5500 V, collision gas MEDIUM, the temperature of ion source at 400°C). The following transitions were monitored: transition 330 to 136 m/z for cAMP (retention time of 2.44 min), transition 346 to 152 m/z for cGMP (retention time of 0.95 min), transition 331 to 137 m/z for cIMP (retention time of 0.98 min). Data were acquired and analysed with Analyst version 1.5.1 (AB Sciex) (Detremmerie et al., 2016).

2.6 | Expression and purification of human soluble guanylyl cyclase (sGC)

Recombinant human α1β1 sGC was expressed in Sf9 cells (RRID: CVCL_0549) and purified to homogeneity as described previously (Chauhan et al., 2012). cGMP forming activity of sGC was assayed by the formation of [³²P] cGMP from α [³²P]GTP at 37°C as described previously (Sharina et al., 2015). In short, 0.2-μg sGC was treated for 10 min at room temperature with freshly prepared NaHS at indicated concentrations or PBS as control. After incubation, the enzyme was added to reaction buffer containing 25-mM triethylammine, pH 7.5, 1 ml·min⁻¹ BSA, 1-mM cGMP, 3-mM MgCl₂, 0.05 ml·min⁻¹ creatine phosphokinase and 5-mM creatine phosphate with or without NaHS and incubated at 37°C for 1 min. The reaction was initiated by adding GTP/α [³²P] GTP mix to the reaction mixture. To determine the GTP-Km, the assay was performed for 10 min at different concentrations of GTP (4–1000 μM) in the absence or presence of NO donor DEA-NO at 10 μM. The reactions were stopped by zinc acetate and processed as described previously (White, 1974) to determine cGMP-forming activity.

The cIMP-forming activity of sGC was assayed as follows. After 10 min of incubation with NaHS or PBS, the enzyme was transferred to the reaction buffer described above and incubated at 37°C for 1 min. To determine the inosine triphosphate-Km (ITP), the assay was
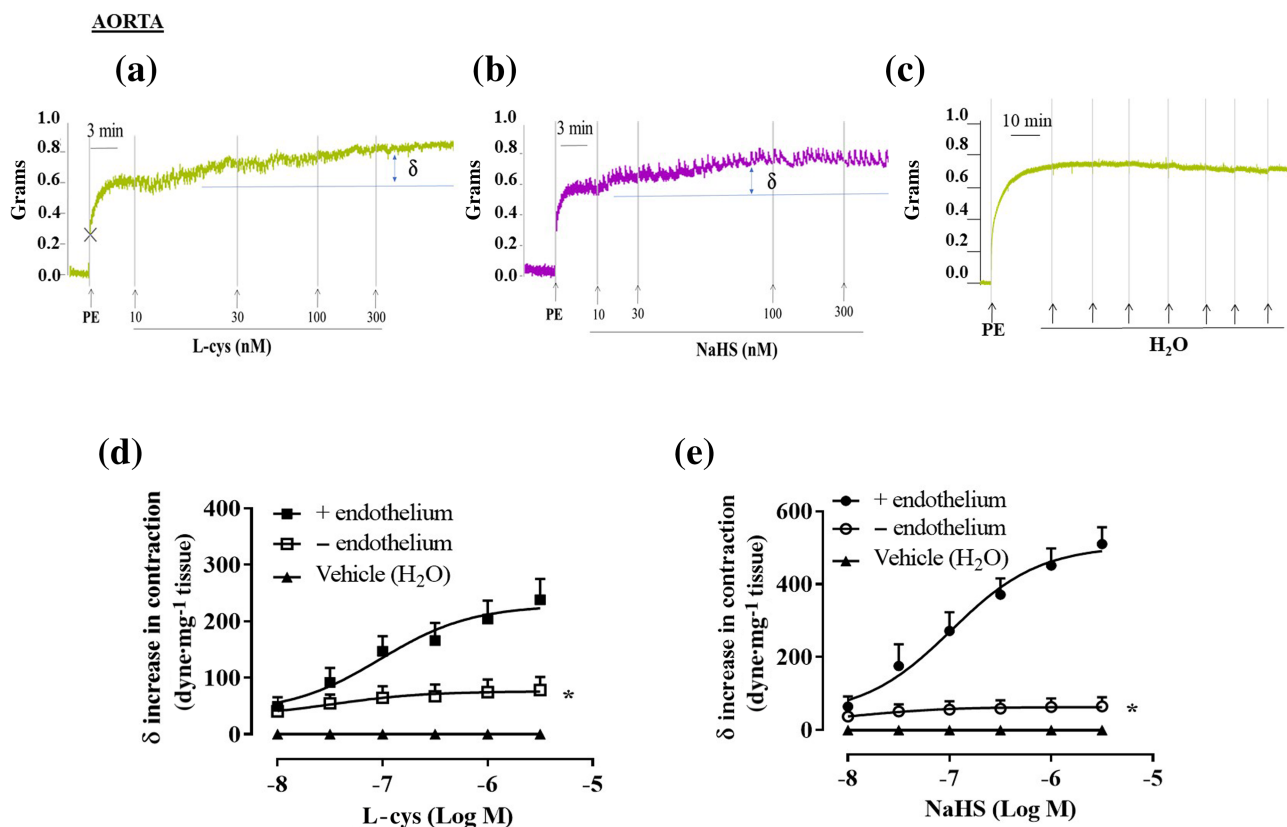
FIGURE 1　L-cysteine and NaHS cause a further increase in tension of phenylephrine (PE)-contracted mouse aortic rings. Representative traces of concentration–response curves induced by (a) L-cysteine (10–300 nM), (b) NaHS (10–300 nM) or (c) vehicle (H₂O) on a stable tone of PE (1 μM). The increase in contraction was blunted by the mechanical endothelium removal for both (d) L-cysteine ($n = 10$ mice) and (e) NaHS ($n = 7$ mice). Values shown are means ± SEM and expressed as δ increase in tension over PE contraction (dyne/mg tissue). *$P < 0.05$ significantly different as indicated; two-way ANOVA with Bonferroni's post hoc test

performed at different concentrations of ITP (4–1000 μM) with or without 10-μM DEA-NO. After 10 min at 37°C, the reactions were stopped by 1-min heat inactivation at 98°C and the denatured protein was removed by 15 min centrifugation at 14000×*g*. The supernatant containing the reaction product was collected and separated by using HPLC Waters Delta 600 instrument equipped with 717Plus Auto-sampler on a Symmetry C18 3.5 μm column (4.6 × 75 mm). ITP and cIMP were separated during the 4-ml gradient run at 1 ml·min⁻¹ from buffer A (50-mM ammonium acetate in 3% methanol and 0.1% acetic acid) to 20% of buffer B (50-mM ammonium acetate in 97% methanol and 0.1% acetic acid) and detected by ultraviolet (UV) at 260 nm. ITP was eluted in the first minute of chromatography, while cIMP was eluted at the 3-min mark. The height and areas of the ITP and cIMP peaks were determined by applying the integration algorithm of the Waters Empower Pro software. The peak height value was used to determine the amount of cIMP generated during the reaction and calculate cIMP-forming activity.

2.7 | Synthesis of cIMP butyrate

cIMP butyrate (2, Scheme 1) has been synthesized by esterification of commercially available inosine 3′-5′-cyclic monophosphate sodium salt 1 with butyric anhydride in the presence of triethylamine in anhydrous pyridine as previously described with some modifications (Posternak & Weimann, 1974).

2.8 | 2-hydroxy-2-oxido-6-(6-oxo-3*H*-purin-9(6*H*)-yl)tetrahydro-4*H*-furo-[3,2-d][1,3,2]dioxa-phosphinin-7-yl butyrate (2)

Commercially inosine 3′-5′-cyclic monophoshate sodium salt (1) (0.5 g, 1.42 mmol) was dissolved in anhydrous pyridine (25 ml) in a two-neck flask and trietylamine (2,41 ml, 17.3 mmol) was added followed by butyric anhydride (3,.7 ml, 18.7 mmol). The mixture was stirred at room temperature for 48 h. The reaction was monitored by TLC (CHCl₃/MeOH/H₂O, 5:4:1); 4 ml of water was added and the solvent was then evaporated under reduced pressure. The residue was prelim-inarily purified by silica gel column chromatography (CHCl₃/MeOH 7:3 [v/v]). The obtained fractions were evaporated and further puri-fied by RP-HPLC. The collected fractions were lyophilized yielding 0.398 g of compound 2 as a white solid. Yield: 70%. m.p. 72°C to 73°C. ESI-MS (negative mode): 399.1. ¹H-NMR (DMSO-d₆): δ 12.53 (bs, 1H, NH), 8.31 (s, 1H), 8.13 (d, *J* = 2.3 Hz, 1H), 6.24 (s, 1H), 5.74 (d, *J* = 5.8 Hz), 5.15–4.54 (m, 1H), 4.24–4.13 (m, 2H), 2.43 (t, 2H, *J* = 7.3 Hz), 1.60 (m, 2H), 0.92 (t, 3H, *J* = 7.3 Hz, CH₃).

2.9 | Randomization, blinding and normalization

Experiments were performed by different operators and animals were randomly used to set up control and experimental groups. Drug treatments were randomized each day of the experiment. Experi-ments were performed by one operator and analysis was carried out by a second one in a blind approach. Data were not normalized and were expressed as absolute values as they were obtained except for data in the following figures: Figure 5f (OD values standardized towards housekeeping protein β-actin); Figures 8c and 9a–c (values expressed as changes over basal production to control for unwanted sources of variation).
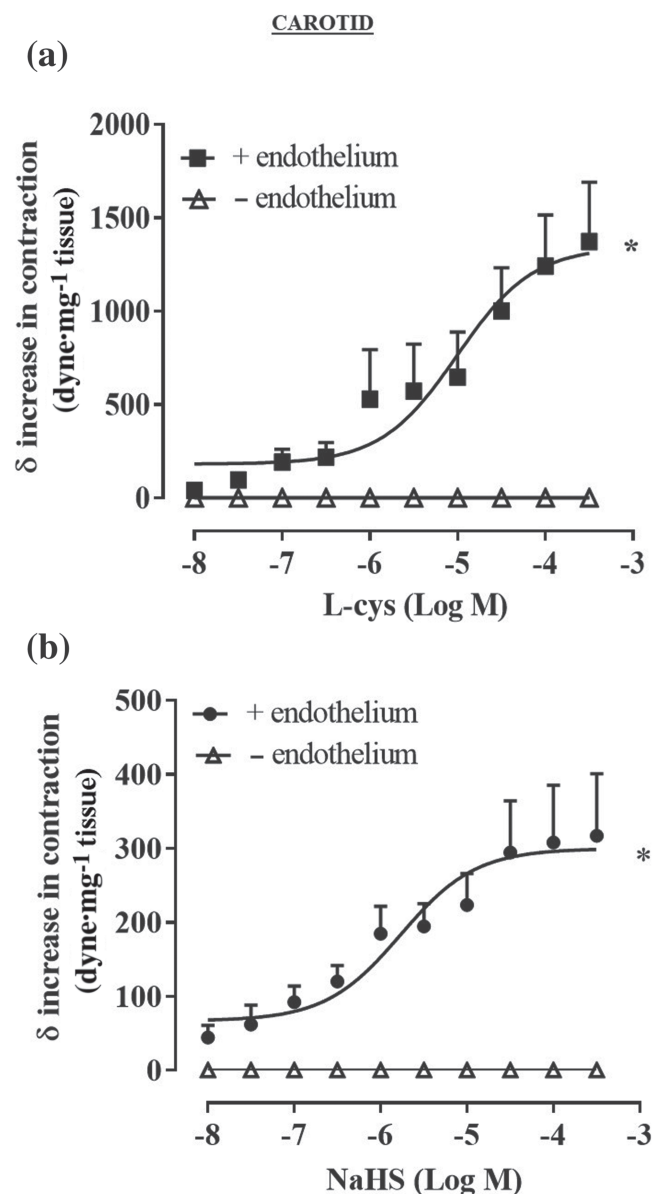
FIGURE 2 L-cysteine and NaHS cause a further increase in tension of phenylephrine (PE)-contracted mouse carotid artery rings. Concentration–response curve of (a) L-cysteine (10 nM to 300 μM) and (b) NaHS (10 nM to 300 μM) on a stable tone of PE (1 μM). The increase in contraction was blunted by the mechanical endothelium removal for both L-cysteine (*n* = 6 mice) and NaHS (*n* = 6 mice). Values shown are means ± SEM and expressed as δ increase in tension over PE contraction (dyne/mg tissue). *$P < 0.05$ significantly different as indicated; two-way ANOVA with Bonferroni's post hoc test

2.10 | Unequal group sizes

The group size was not equal for all experiments, as detailed in the figure legends. In some cases, n for control groups is higher than 5 since the controls have been repeated in all animal experiments. In addition, the procedure does not allow to run the whole set of treatments for each type of test.

2.11 | Data and statistical analysis

The data and statistical analysis comply with the recommendations of the British Journal of Pharmacology on experimental design and analysis in pharmacology (Curtis et al., 2018). All data were expressed as mean ± standard error of the mean (SEM). The number of animals used for each data set was $n \geq 5$, as shown in each figure legend. Sample size was based on estimations by power analysis with a level

of significance of 0.05 and a power of 0.85. Statistical analysis was performed by using one-way analysis of variance (ANOVA), followed by Dunnett's post-test, two-way ANOVA followed by Bonferroni's post-test or one-sample t-test where appropriate. Bonferroni's post hoc test was run only when F was significant. Prism 7.0 software (GraphPad, San Diego, CA, USA, RRID:SCR_002798) was used to analyse all data set and perform statistics. P values < .05 were indicative of statistical significance for all comparisons.

2.12 | Materials

NaCl, KCl, $MgCl_2$, KH_2PO_4, $CaCl_2$, $NaHCO_3$, glucose, NaHS, L-cysteine, phenylephrine, ACh, 5-HT, L-NIO (N^5-(1-Iminoethyl)-L-ornithine dihydrochloride), Tris-HCl, sodium deoxycholate, sodium dodecyl sulfate, EDTA, Igepal, protease inhibitor cocktail, BSA, Tween 20, β-actin, methanol, ammonium acetate, acetic acid, creatine
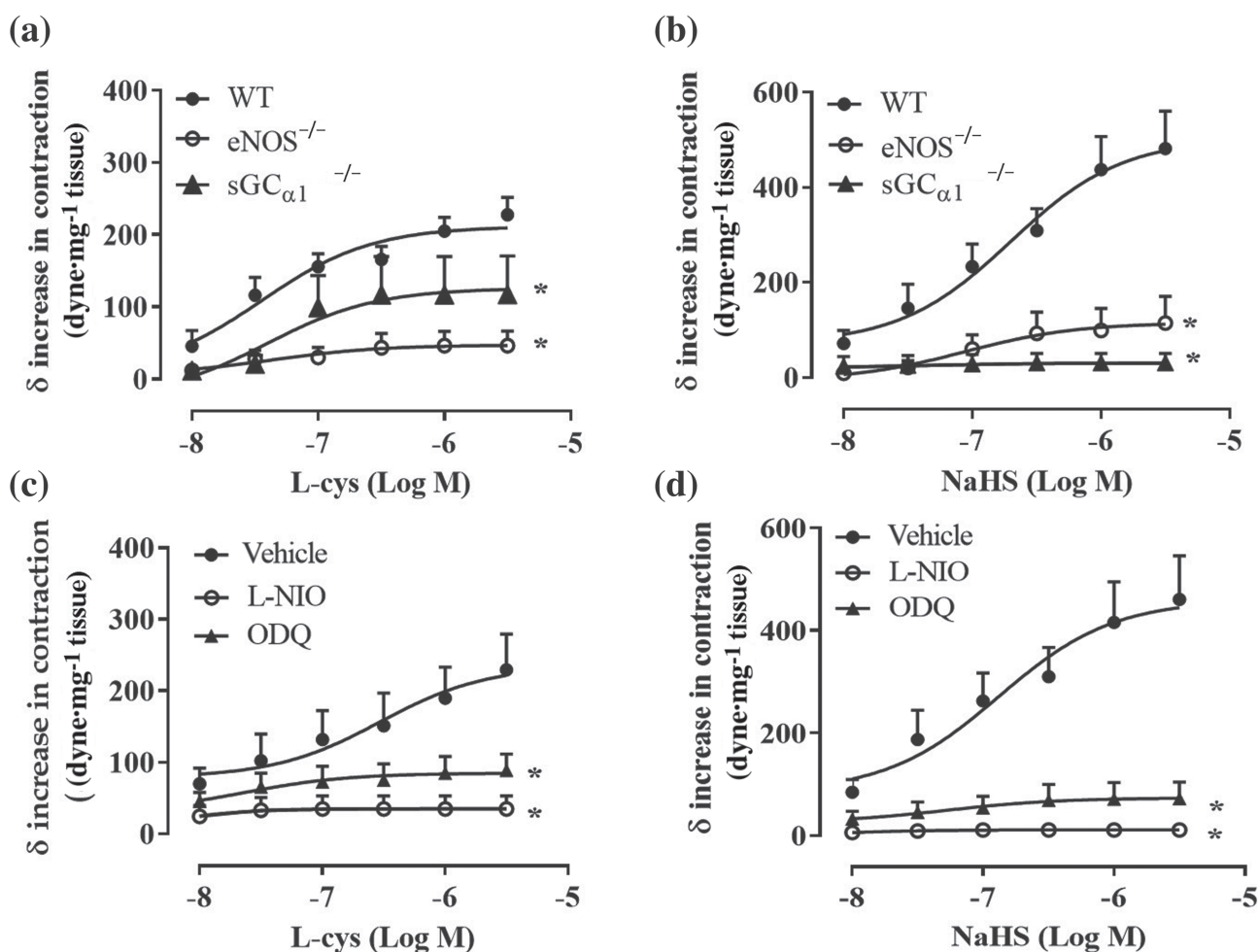
FIGURE 3 L-cysteine- and NaHS-induced increase in tension involves the eNOS/sGC/NO pathway. (a) L-cysteine- and (b) NaHS-induced contraction on phenylephrine (PE)-precontracted aortic rings was abolished in aorta harvested from eNOS$^{-/-}$ ($n = 7$ mice L-cysteine, $n = 6$ mice NaHS) and sGC$_{\alpha 1}$$^{-/-}$ mice ($n = 7$ mice L-cysteine, $n = 9$ mice NaHS) compared to WT mice ($n = 7$ mice L-cysteine, $n = 9$ mice NaHS). (c) L-cysteine-induced contraction is abolished in PE-precontracted aortic rings incubated with L-NIO (10 μM, 20 min; $n = 5$ mice) or ODQ (10 μM, 15 min; $n = 8$ mice) compared to vehicle ($n = 8$ mice). (d) NaHS-induced contraction is abolished in PE-precontracted aortic rings incubated with L-NIO (10 μM, 20 min; $n = 6$ mice) or ODQ (10 μM, 15 min; $n = 6$ mice) compared to vehicle ($n = 8$ mice). Values shown are means ± SEM and are expressed as δ increase in tension over PE contraction (dyne/mg tissue). *P < 0.05 significantly different as indicated; two-way ANOVA with Bonferroni's post hoc test

phosphokinase, creatine phosphate DEA-NO, zinc acetate and, inosine triphosphate and stock solution of cGMP, cAMP and cIMP were supplied by Sigma-Aldrich, (Milan, Italy). Inosine 3′-5′-cyclic monophoshate sodium salt was supplied by (Merck, Germany). Anti-p-PDE4A and anti-p-PDE5 were supplied by Fabgennix (Frisco, TX, USA). Anti-PDE4A was supplied by ProteinTech (Manchester, UK). Anti-PDE5 was supplied by Santa Cruz Biotechnology (Heidelberg, Germany). Anti-eNOS was supplied by BD Transduction Laboratories (USA). Anti-β-actin was supplied by Merck (Germany). ODQ, U46619, FR 139317 and BQ788 were supplied by Tocris (Bristol, UK).

2.13 | Nomenclature of targets and ligands

Key protein targets and ligands in this article are hyperlinked to corresponding entries in the IUPHAR/BPS Guide to PHARMACOLOGY http://www.guidetopharmacology.org and are permanently archived in the Concise Guide to PHARMACOLOGY 2019/20 (Alexander et al., 2019).

3 | RESULTS

3.1 | Nanomolar concentrations of H_2S induce further vasoconstriction of phenylephrine precontracted aorta and carotid arteries

In isolated aortic rings, L-cysteine or NaHS addition on basal tone *per se* does not cause any significant change in tension (Figure S1A,B). Upon stimulation with the α_1-adrenoceptor agonist phenylephrine, once a stable contraction was achieved, administration of either L-cysteine (Figure 1a) or NaHS (Figure 1b) induces a further increase in tension. Vehicle (H_2O) administration on phenylephrine precontracted rings did not cause any additional contraction (Figure 1c). The contractile effect observed with L-cysteine and NaHS is endothelium dependent and restricted within a specific low range of concentration (10 nM to 1 μM) (Figure 1d,e). When aortic rings have been obtained from mice younger than 20 weeks, both L-cysteine (10 nM to 300 μM) and NaHS (10 nM to 300 μM) fail to induce contraction showing exclusively vasodilating activity at high concentrations (Figure S1C,D). Therefore, all subsequent studies have been performed on mature adult mice of at least 20 weeks of age. A similar profile has been obtained using isolated carotid rings (Figure 2). Indeed, both L-cysteine (Figure 2a) and NaHS (Figure 2b) induce a further increase in tension on a background of stable phenylephrine induced tone.

3.2 | The eNOS/NO/sGC pathway plays an obligatory role in H_2S contractile effect

To evaluate the contribution of eNOS/NO/sGC pathway in H_2S-induced contraction, the same protocol described above has been performed on aorta harvested from eNOS$^{-/-}$ and sGC$_{\alpha1}$$^{-/-}$

mice. sGC$_{\alpha1\beta1}$ is the most abundant isoform within the vasculature (Mergia et al., 2006; Vellecco et al., 2016) and it has been shown that mice lacking sGC$_{\alpha1}$ develop hypertension (Mergia et al., 2006). As shown in Figure 3a,b, the absence of eNOS, as well as sGC$_{\alpha1}$, abrogates both L-cysteine and NaHS-induced contraction elicited over phenylephrine-induced tone. This finding suggests a key role for eNOS/NO/sGC signalling in H_2S-induced contraction. This result has
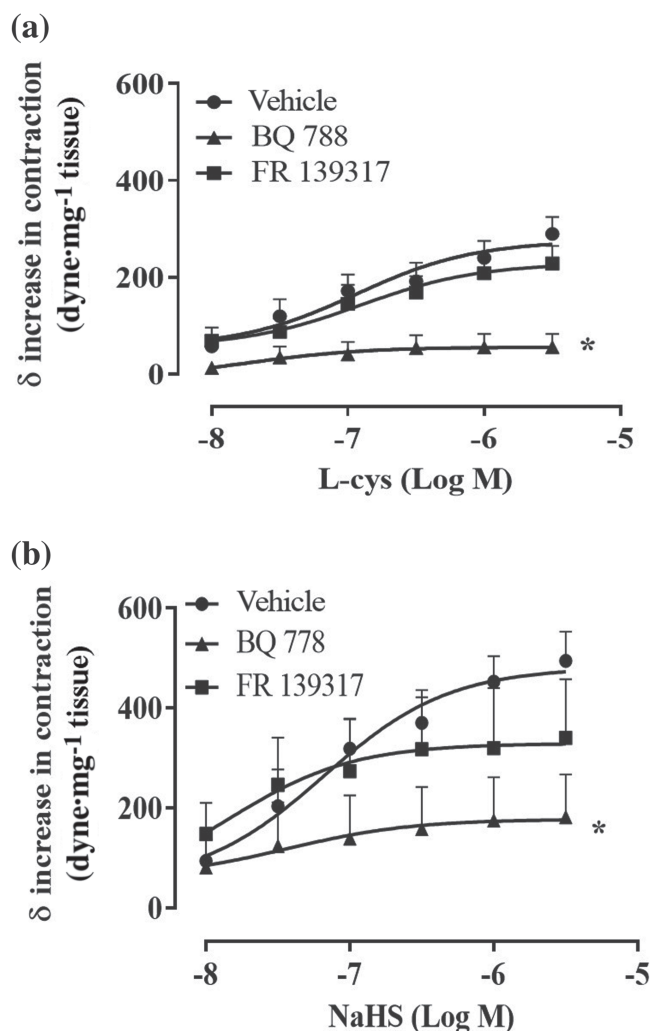
FIGURE 4 L-cysteine- and NaHS-induced increase in tension do not involve endothelin-1. (a) L-cysteine and (b) NaHS concentration–response curves are performed on the stable tone induced by phenylephrine (PE) in the presence of selective ET receptor subtype antagonists. Selective inhibition of ET$_A$ (mainly expressed on smooth muscle component) by FR 139317 (1 nM, 20 min) does not affect L-cysteine- and NaHS-induced contraction compared to vehicle ($n = 8$ mice). Selective inhibition of ET$_B$ receptor (expressed mainly on endothelium whose activation induces NO release) by BQ788 (10 μM, 20 min), significantly reduces L-cysteine- and NaHS-induced contraction compared to vehicle ($n = 8$ mice). Values shown are means ± SEM and are expressed as δ increase in tension over PE contraction (dyne/mg tissue). *$P < 0.05$ significantly different compared to vehicle, two-way ANOVA with Bonferroni's post hoc test

been confirmed by the pharmacological inhibition of eNOS and sGC in aorta harvested from WT mice. Indeed, incubation of the rings with L-NIO, a selective eNOS inhibitor, or ODQ, a NO-sensitives GC inhibitor, blunts both L-cysteine and NaHS-induced contraction over phenylephrine bachground tone (Figure 3c,d). One of the most widely known contractile factors released by the vasculature is endothelin-1 (ET-1) (Davenport et al., 2016; Dhaun & Webb, 2019). To rule out its possible contribution that an endothelium-derived contractile mediator is involved in H_2S-induced contraction, *in vitro* experiments with the selective ET receptor subtype antagonists have been performed. FR139317, a selective antagonist of ET_A receptor, which is mainly expressed on smooth muscle cells (Miyauchi & Masaki, 1999), does not affect L-cysteine (Figure 4a) or NaHS-induced contraction (Figure 4b), excluding ET-1 involvement in H_2S-induced vasoconstriction (Mazzuca & Khalil, 2012). Conversely, BQ778, a selective antagonist of ET_B receptor, which is mainly expressed on the endothelium and coupled to NO release (Maguire & Davenport, 1999), abolished H_2S-induced contraction (Figure 3a,b). This evidence further supports the essential role of NO in H_2S-induced contraction.

3.3 | $CSE^{-/-}$ mice aorta and carotid arteries display impaired vasoconstriction

To further dissect the role of H_2S in vascular contractility, the reactivity of aorta isolated from $CSE^{-/-}$ mice has been evaluated. As shown in Figure 5, aortic rings harvested from $CSE^{-/-}$ mice display a marked impaired vasoconstriction in response to phenylephrine, compared to WT mice (Figure 5a–c). To evaluate whether the hypocontractility observed is due to changes in eNOS function and/or expression, two different experiments have been performed:- (i) a cumulative concentration–response to phenylephrine on $CSE^{-/-}$ mice aorta in the presence of L-NIO, a selective eNOS inhibitor and (ii) western blot analysis on $CSE^{-/-}$ mice aorta to detect eNOS expression. As shown in Figure 5, neither L-NIO affects phenylephrine-induced contraction (Figure 5d,e) nor western blot analysis (Figure 5f) reveals any difference in eNOS expression between $CSE^{-/-}$ and WT mice. These results indicate that, in $CSE^{-/-}$ mouse aorta, the eNOS pathway is not affected by CSE gene deletion. To better characterize its vascular reactivity, both $CSE^{-/-}$ aortic and carotid rings have been challenged with
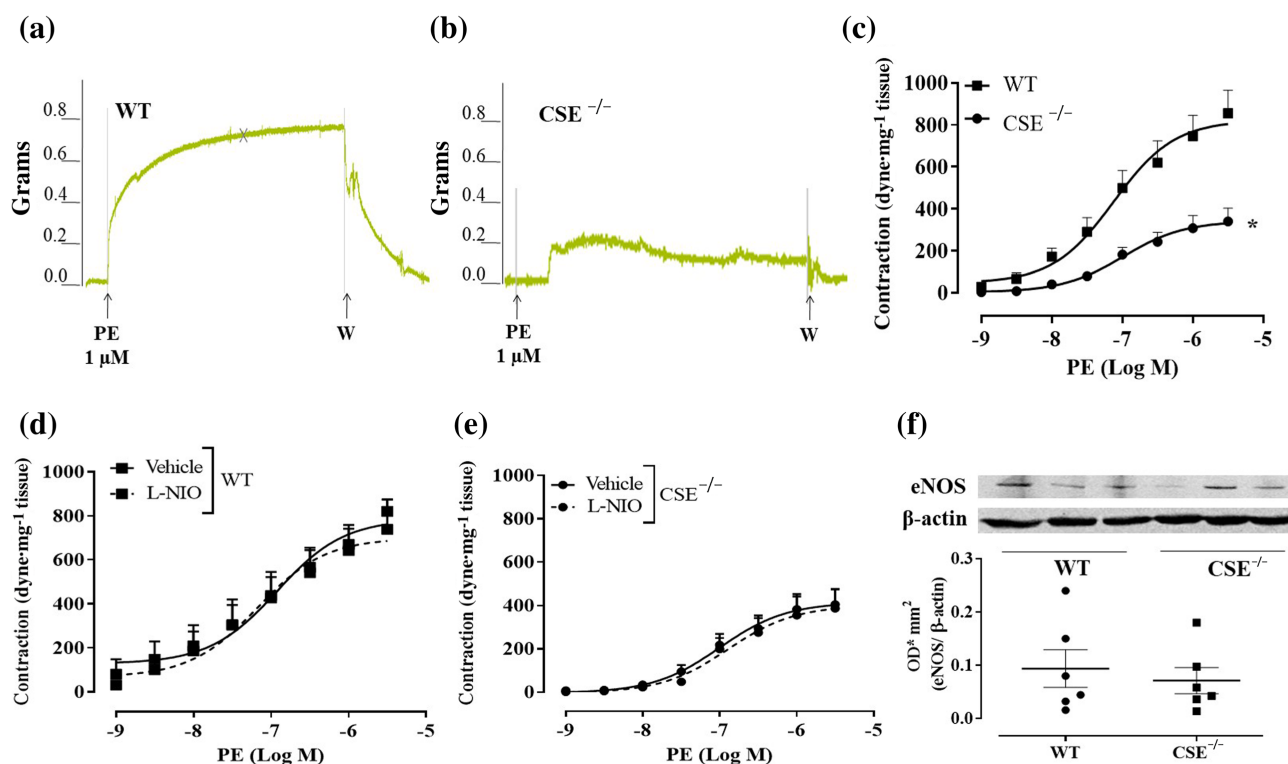
FIGURE 5 Aortas of $CSE^{-/-}$ mice displays vascular hyporeactivity to phenylephrine (PE) and an unmodified NO signalling. Representative traces of PE-induced contraction in aortic rings harvested from (a) WT mice and (b) $CSE^{-/-}$ mice. $CSE^{-/-}$ mice display a reduced level of contraction compared to WT mice. (c) the cumulative concentration–response curve to PE on aorta of $CSE^{-/-}$ mice ($n = 10$ mice) is significantly reduced compared to WT mice ($n = 7$ mice). (d) Concentration–response curve to PE performed on aortic rings harvested from WT mice. The incubation with L-NIO (10 μM, 20 min), the eNOS selective inhibitor, does not affect PE-induced contraction ($n = 7$ mice). (e) Concentration–response curve to - performed on aortic rings harvested from $CSE^{-/-}$ mice. The incubation with L-NIO (10 μM, 20 min), the eNOS selective inhibitor, does not affect PE-induced contraction ($n = 7$ mice). Values shown are means ± SEM and are expressed as a contraction (dyne/mg tissue). *$P < 0.05$ significantly different as indicated; two-way ANOVA with Bonferroni's post hoc test. (f) Representative western blot analysis (upper) and densitometric analysis (lower) for eNOS expression in aorta of WT and $CSE^{-/-}$ mice ($n = 6$ mice). The western blot study does not reveal a significant difference in eNOS expression between WT and $CSE^{-/-}$ mice; Student's *t*-test

other contracting agents besides phenylephrine, that is, 5-HT, U46619 (a thromboxane analogue) and KCl (a depolarizing agent). Data obtained from aortic rings are shown in Figure 6, while data obtained for carotid rings are shown in Figure 7. All agents tested induce contractile responses significantly weaker than those observed in WT mice arteries. These data suggest that in $CSE^{-/-}$ mice, the lack of CSE-derived H_2S leads to a generalized hyporeactivity that is unrelated to the contractile stimulus.

## 3.4 | cAMP, cGMP and cIMP levels are altered in $CSE^{-/-}$ mice aorta

Among the cyclic nucleotides, cIMP has been shown to exert vasocontraction (Chen et al., 2014; Detremmerie et al., 2016). cIMP is the first, in terms of levels detected, of the minor products of sCG (Beste et al., 2012; Chen et al., 2014) and its biosynthesis requires the endothelium-derived NO activation of sGC (Leung et al., 2017). The homogenised aorta samples from either WT or $CSE^{-/-}$ mice were processed to detected simultaneously cIMP, cGMP and cAMP levels by using UPLC-MS/MS analysis (Figure 8a,b). All measurements are summarized in Figure 8c and show that cIMP is virtually absent in $CSE^{-/-}$ mouse tissues (below the detection limit).

## 3.5 | H_2S modifies cyclic nucleotides ratio in wild type mice aorta

To define if the increase in contraction over the level of phenylephrine induced stable tone elicited by low concentration of H_2S does involve cIMP, the levels of the cyclic nucleotides, that is, cAMP, cGMP and cIMP have been measured in WT mice aorta incubated with NaHS (1 μM) for 5 or 15 min. The concentration of 1 μM has been chosen since it is the highest concentration that induces contraction, while 5–15 min is the timeframe necessary to achieve the maximal increase in tension *in vitro*. Under these conditions, NaHS (1 μM) reduces both cAMP and cGMP levels. In particular, following 5 min of incubation, NaHS induces a significant drop in cGMP by 19% (Figure 9a). This reduction lasts up to 15 min post-NaHS exposure. A similar profile is displayed for cAMP, where NaHS (1 μM) significantly reduces the levels of cAMP either to 5 and 15 min leading to an inhibition of 14% and 22%, respectively (Figure 9b). Conversely, the incubation of vessels with NaHS (1 μM) induces an increasing trend for cIMP of 16% following 5 and 15 min of exposure (Figure 9c). The reduction observed for both cGMP and cAMP falls within the same range of cIMP increase, that is, 15–20%. Therefore, the transient reduction of both cAMP and cGMP, coupled with the cIMP increase driven by H_2S, leads to the endothelium-dependent contractile effect.
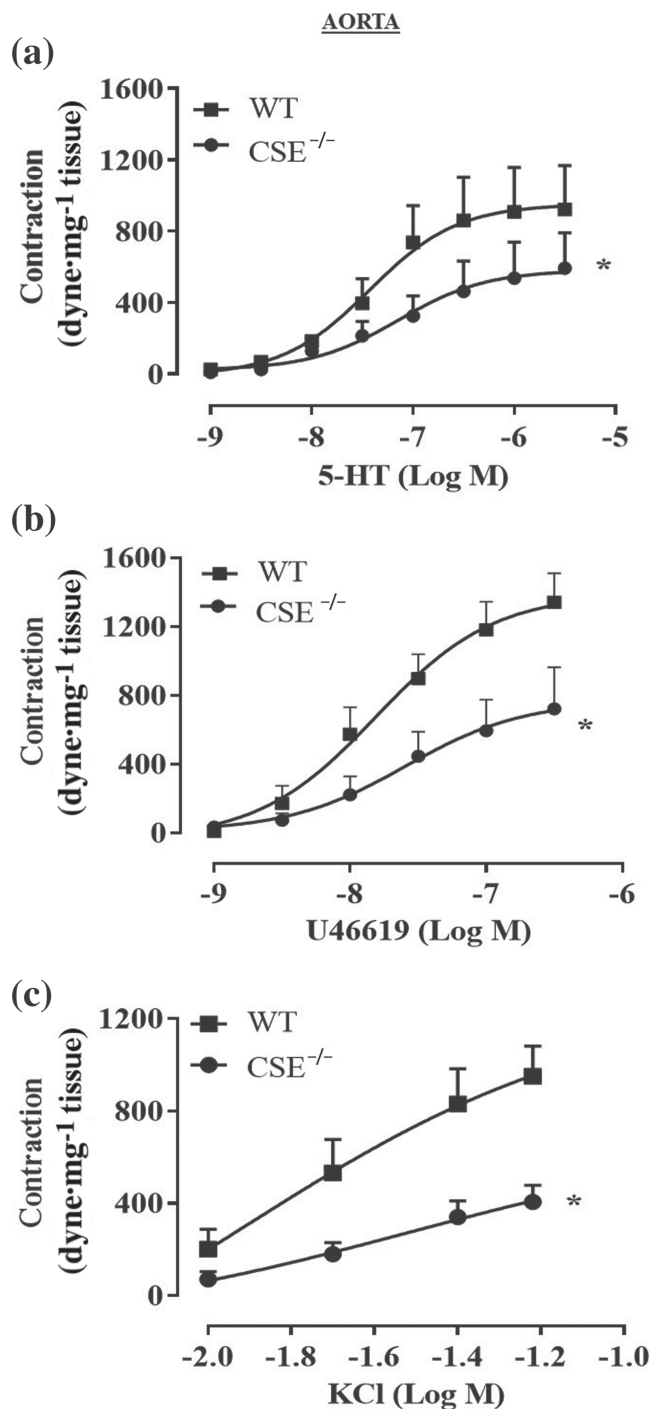
FIGURE 6 Aortas of $CSE^{-/-}$ mice display a generalized hyporeactivity to different agonists. Cumulative concentration–response curves performed with (a) 5-HT (1 nM to 3 μM; $n = 5$ WT and $n = 5$ $CSE^{-/-}$ mice), (b) U46619 (1 nM to 0.3 μM; $n = 6$ WT and $n = 6$ $CSE^{-/-}$ mice) or (c) KCl (10, 20, 40, 60 mM; $n = 9$ WT and $n = 12$ $CSE^{-/-}$ mice) were significantly reduced in $CSE^{-/-}$ mice compared to WT mice. Values shown are means ± SEM and are expressed as contraction (dyne/mg tissue). *$P < 0.05$ significantly different compared to WT mice; two-way ANOVA with Bonferroni's post hoc test
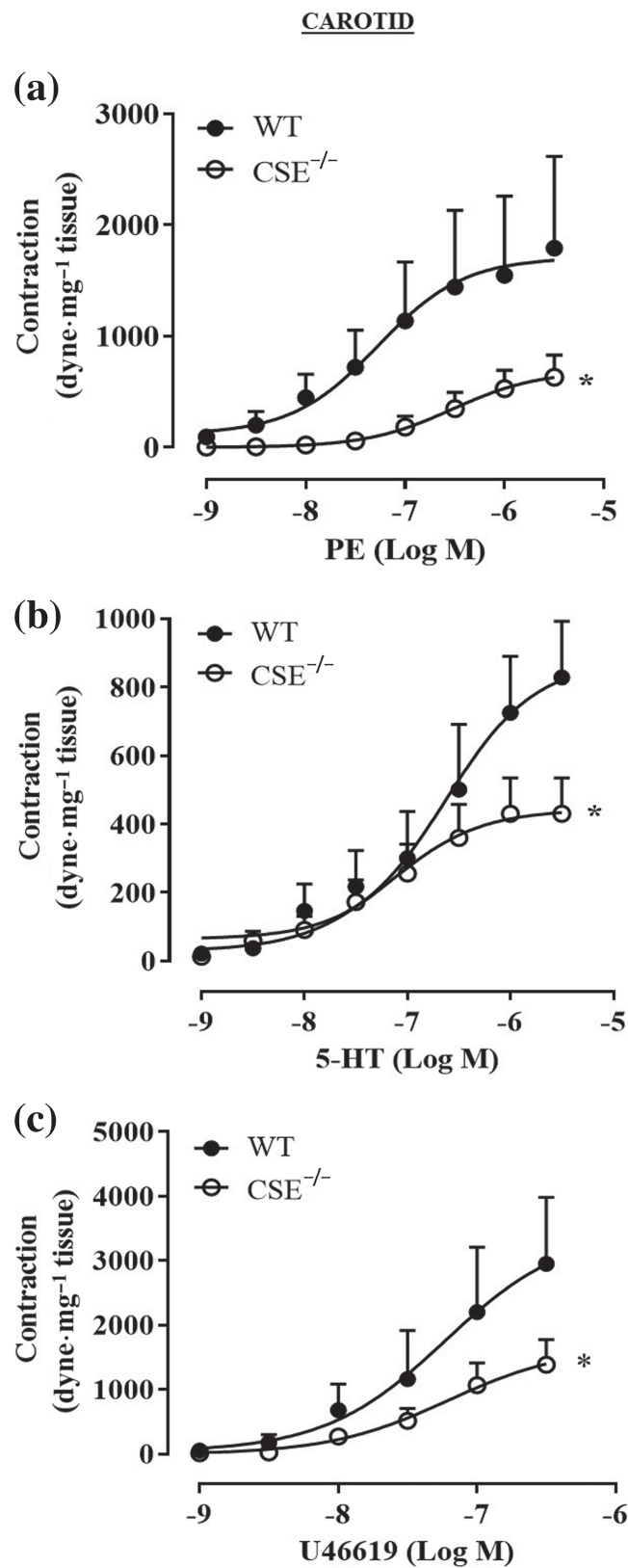
CAROTID

FIGURE 7 Carotid arteries of CSE$^{-/-}$ mice display a generalized hyporeactivity to different agonists. Cumulative concentration–response curves performed with (a) phenylephrine (PE; 1 nM to 3 μM; $n = 7$ WT and $n = 8$ CSE$^{-/-}$ mice), (b) 5-HT (1 nM to 3 μM; $n = 5$ WT and $n = 9$ CSE$^{-/-}$ mice), (c) U46619 (1 nM to 0.3 μM; $n = 5$ WT and $n = 8$ CSE$^{-/-}$ mice) were significantly reducted in CSE$^{-/-}$ mice compared to WT mice. Values shown are means ± SEM and are expressed as contraction (dyne·mg^{-1} tissue). *$P < 0.05$ significantly different compared to WT mice; two-way ANOVA with Bonferroni's post hoc test
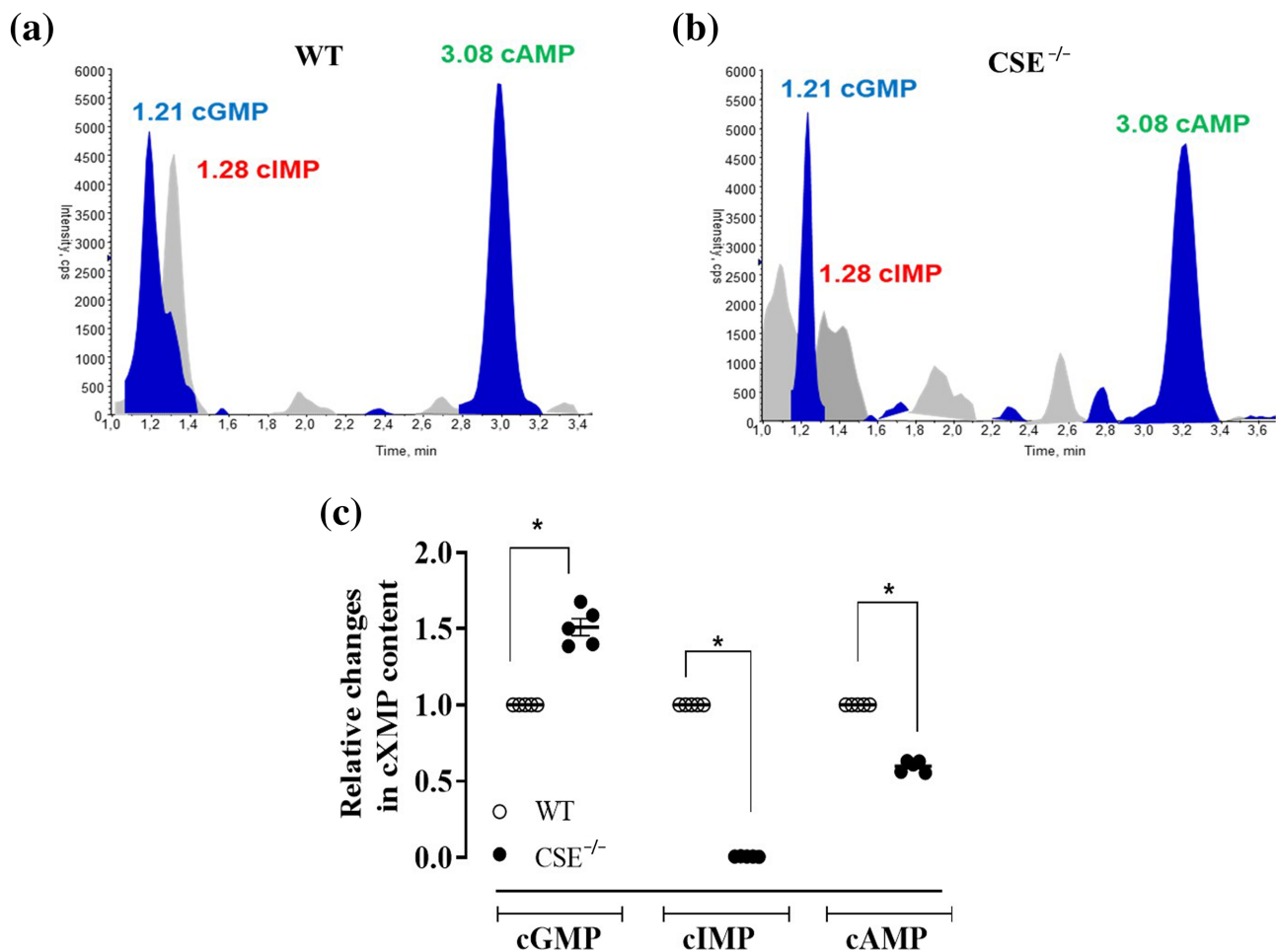
FIGURE 8 The relative content of cyclic nucleotides in the aorta of CSE$^{-/-}$ mice and WT mice. The cyclic nucleotides levels are detected simultaneously in homogenates of mouse aortas using UPLC-MS/MS. typical trace analysis of the determination of the cyclic nucleotides in (a) WT and (b) CSE$^{-/-}$ mice. The cyclic nucleotide levels in WT are 261.99 ± 9.36 (cAMP), 9.13 ± 0.89 (cGMP), 19.87 ± 6.43 (inosine 3′,5′-cyclic monophosphate/cIMP) pg/mg tissue. The cyclic nucleotides levels in CSE$^{-/-}$ mice are 156.38 ± 5.51 (cAMP), 13.31 ± 0.63 (cGMP), 0.18 ± 0.02 (cIMP) pg/mg tissue. (c) the data are expressed as a relative change compared to the levels of cyclic nucleotides detected in WT aorta, taken as 1. Values shown are means ± SEM; $n = 5$ determinations (three mouse aortas are pulled in each sample). *$P < 0.05$ significantly different as indicated; one-way ANOVA with Bonferroni's post hoc test

3.6 | NaHS at nanomolar concentration does not modify purified recombinant sGC activity *in vitro*

A possible underlying mechanism in altered cyclic nucleotide levels could be that nanomolar concentration of NaHS exhibit biased agonist properties leading to preferred cIMP synthesis over cGMP. To test this hypothesis, purified recombinant sGC has been used and sGC activity monitored supplying GTP or ITP as substrates. sGC exhibits low basal cGMP and cIMP forming ability that is significantly stimulated by NO addition (Table 1). Although nanomolar concentrations of NaHS increase the affinity of sGC for ITP, this is not reflected by changes in the cIMP-forming ability of sGC, as V_{max} is similar in the presence or absence of 300-nM NaHS. High concentrations of NaHS (300 μM) have effects on neither K_m nor V_{max} when ITP is used as a substrate (Table 1). Instead, when the substrate used is GTP, both low and high NaHS concentrations increase basal sGC activity but caused a marginal drop in NO-stimulated sGC activity.

The small decrease in the cGMP-forming activity of sGC in the presence of 300-nM NaHS is in line with the drop in cGMP levels observed in tissue treated with the low concentration of NaHS (Figure 9a).

3.7 | NaHS at nanomolar concentration modulates PDE4A and PDE5 activity

The lack of effect on purified recombinant sGC leads us to investigate if the nanomolar concentration of H$_2$S could alter cAMP and cGMP breakdown. We evaluated the activity of PDE4A (cAMP-specific) and PDE5 (cGMP specific) by measuring pPDE/PDE ratio, in WT mice aorta incubated with NaHS 1 μM, as an index of enhanced PDE activity (Francis et al., 2011). Western blot analysis shows that, following NaHS stimulation, both pPDE4A/PDE4A and pPDE5/PDE5 ratios significantly increase after 5 min of incubation, lasting up to 15 min
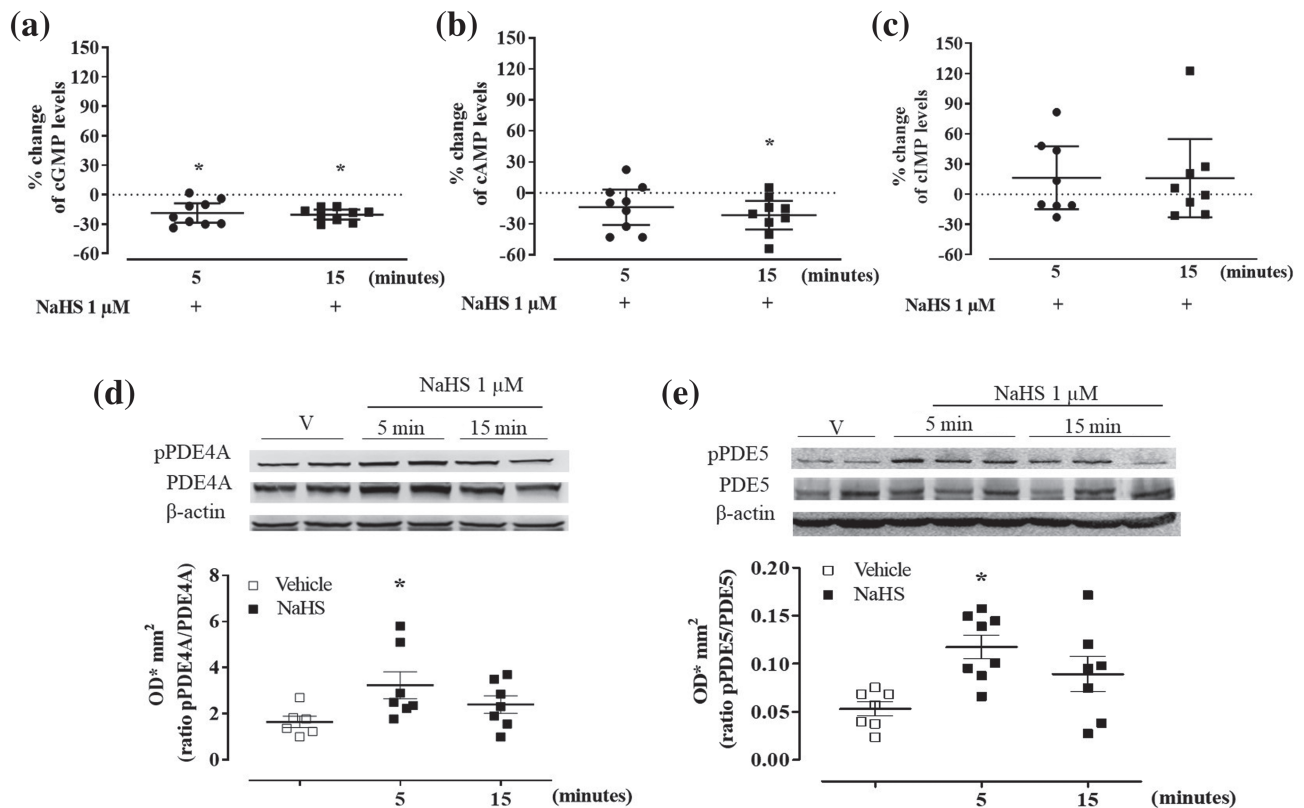
FIGURE 9 NaHS (1 μM) modulates cyclic nucleotides through PDEs activity in WT mice aorta. Following 5 and 15 min of incubation, NaHS induces (a) significant reduction of cGMP content of 18.7% and 20.3%, compared to the respective vehicle that is 18.58 ± 2.43 pg·mg^{-1} tissue (n = 9 determinations), (b) significant reduction of cAMP content of 13.9% and 21.7%, compared to the respective vehicle that is 153.87 ± 6.02 pg·mg^{-1} tissue (n = 9 determinations) and (c) trend of increase in inosine 3′,5′-cyclic monophosphate (cIMP) levels of 16.4% and 15.7%, compared to the respective vehicle that is 5.41 ± 1.05 pg·mg^{-1} tissue (n = 8 determinations). Values shown are means ± SEM n = 9 determinations or 8 determinations (three mouse aortas are pulled in each sample) and are expressed as the percentage of change compared to the level measured in the vehicle. *$P < 0.05$ significantly different; one sample t-test. (d) Upper: Representative western blot for pPDE4A and PDE4A expression in homogenates of aorta incubated with NaHS (1 μM) for 5 or 15 min or vehicle (V). Lower: Densitometric analysis of pPDE4A/PDE4A ratio. The ratio pPDE4A/PDE4A is significantly enhanced following NaHS incubation at 5 min compared with vehicle (vehicle n = 6 mice; 5 and 15 min n = 7 mice). (e) Upper: Representative western blot for pPDE5 and PDE5 expression in homogenates of aorta incubated with NaHS (1 μM) for 5, 15 min or vehicle. Lower: Densitometric analysis for pPDE5/PDE5 ratio. The ratio pPDE5/PDE5 is significantly enhanced following NaHS incubation at 5 min compared with vehicle (vehicle n = 7 mice; 5 min n = 8 mice; 15 min n = 7 mice). Values shown are means ± SEM and are expressed as optical densitometric (ODmm^2). *$P < 0.05$ significantly different compared to the vehicle; one-way ANOVA with Bonferroni's post hoc test

(Figure 9d,e). This timeframe fits well with the reduction in cGMP and cAMP that unmasks the cIMP effect. Thus, nanomolar concentrations of NaHS promote PDEs phosphorylation enhancing cyclic nucleotide catabolism.

3.8 | Nanomolar concentrations of cIMP butyrate induce further vasoconstriction of phenylephrine precontracted aorta

In isolated aortic rings, cIMP butyrate (Figure 10a) does not modify the basal tone (Figure 10b). Conversely, upon stimulation with the α_1_adrenoceptor agonist phenylephrine, once a stable contraction is achieved, cIMP butyrate (0.1 nM to 1 μM) induces a further increase in tension that is concentration dependent (Figure 10c).

4 | DISCUSSION

A contractile effect of L-cysteine on blood isolated aorta was already accidentally described in 1993, using the isolated organ bath technique, by Furchgott (Jia & Furchgott, 1993). He found that in phenylephrine-precontracted rings, low concentrations of L-cysteine caused a further increase of tension followed by a relaxing effect at higher concentration. In more recent years, it has been shown that hydrogen sulfide donors or L-cysteine elicit a biphasic activity on isolated precontracted vessels, depending upon the concentration used. Intriguingly, only the contractile effect in phenylephrine-precontracted vessels is endothelium dependent (Kubo et al., 2007; Lim et al., 2008; Liu et al., 2011; Webb et al., 2008). Pharmacological modulation with inhibitors of the eNOS/NO/sGC pathway corroborated the obligatory role for the NO pathway. Indeed, either L-NIO, a

TABLE 1 Effect of NaHS on purified soluble guanylyl cyclase (sGC) with or without NO by using either ITP or GTP as substrates

|	ITP K_m (µM)	ITP V_{max} (µmole min^{-1} mg^{-1})
Basal activity	69.3 ± 27.5	0.084 ± 0.009
With 300-nMNaHS	21.3 ± 8.2*	0.078 ± 0.007
With 300-µM NaHS	96.9 ± 37.7	0.093 ± 0.013
10-µM NO	66.4 ± 11.1	2.86 ± 0.12*
With 300-nMNaHS	62.3 ± 16.5	2.73 ± 0.15
With 300-µM NaHS	94.2 ± 15.7[#]	2.66 ± 0.17[#]
	GTP K_m (µM)	GTP V_{max} (µmole min^{-1} mg^{-1})
Basal activity	154 ± 13.2	0.099 ± 0.005
With 300-nMNaHS	299.8 ± 48.9*	0.166 ± 0.020*
With 300-µM NaHS	149.4 ± 15.1	0.150 ± 0.011*
10-µM NO	44.4 ± 3.8*	6.39 ± 0.13*
With 300-nMNaHS	44.0 ± 7.5*	5.69 ± 0.23*,[#]
With 300-µM NaHS	87.0 ± 19.2*,[#]	5.68 ± 0.22*,[#]

*Statistically significant vs. basal value.
[#]Statistically significant vs. NO-induced value.

selective inhibitor of eNOS, or ODQ, a sGC inhibitor, mimicked the effect observed following the mechanical endothelium removal displayed in phenylephrine-precontracted rings. To further define the role of the eNOS/NO/sGC pathway in this phenomenon, we used aorta harvested from either eNOS$^{-/-}$ or sGC$_{\alpha1}$$^{-/-}$ mice. In phenylephrine-precontracted aortic rings of both mouse strains, hydrogen sulfide fails to induce vasoconstriction, thereby confirming the obligatory role for eNOS/NO/sGC signalling for hydrogen sulfide-induced vasoconstriction. These data imply that under physiological conditions, CSE-derived hydrogen sulfide contributes to the dynamic vessel homeostasis by also modulating the contractile tone. In physiological conditions, vessel tone is mainly determined by the dynamic balance between the endogenous α-adrenoceptor contractile signalling and vasodilating eNOS/NO/sGC pathway. To better define the role played by endogenous CSE-derived hydrogen sulfide in this phenomenon, we used aorta and carotid harvested from CSE$^{-/-}$ mice. At first, we evaluated the ability of these two different types of arteries (capacitance and resistance artery, aorta and carotid respectively) to contract to phenylephrine. We found that CSE$^{-/-}$ mice vessels display a threefold reduction of phenylephrine-induced contraction force. The contraction elicited by phenylephrine is also not very stable, as can be seen in the aorta original experimental traces (Figure 5a,b). The hypocontractility of arteries harvested from CSE$^{-/-}$ mice was not restricted to phenylephrine, but it was also shared with other contractile agents, such as KCl, U46619 and 5-HT, all of which have different signal transduction mechanisms. Such generalized impairment in the contractile response to different agonists reinforces the concept that the endogenous CSE-derived hydrogen sulfide is involved in the modulation of the contractile tone. The finding that in aorta of either wild type or CSE$^{-/-}$ mice (i) the contraction induced by a cumulative concentration–response is not modified by eNOS inhibition and (ii) eNOS expression is not significantly altered rules out

a possible enhancement of NO signalling in CSE$^{-/-}$ hypocontractility. Other than the main cyclic nucleotides, cGMP and cAMP, at least another five cyclic nucleotides are produced by sGC (Beste et al., 2012; Reinecke et al., 2011). Among these cyclic nucleotides, we focused on cIMP since it has been shown to trigger a contraction of the vasculature (Chen et al., 2014; Gao et al., 2015). It has been shown that the increase in cIMP production leads to endothelium-dependent vasoconstriction and, more specifically, NO/sGC pathway dependent (Chen et al., 2014). The first hint for a link among cIMP, vascular contraction and the CSE/hydrogen sulfide pathway has been obtained by analysing the relative abundance of cyclic nucleotides in CSE$^{-/-}$ mice aorta. In these mice, cIMP was undetectable by the assay employed. Thus, the hypocontractility observed in CSE$^{-/-}$mice coupled to the lack of cIMP suggest that the contraction elicited by nanomolar concentrations of hydrogen sulfide in phenylephrine precontracted vessels could involve this cyclic nucleotide, cIMP. To test this hypothesis, we incubated mouse aortas harvested from wild type mice with a low concentration of NaHS. To mimic the organ bath experimental condition, we used as incubation time the same time frame necessary to elicit contraction in phenylephrine-precontracted rings. The data clearly show that nanomolar concentrations of NaHS, which cause a contraction in vitro, negatively modulate the main two cyclic nucleotides involved in the relaxant effect, namely, cGMP and cAMP. This transient reduction of cAMP and cGMP levels unmasks the contractile effect of cIMP. This finding, taken together with the generalized hyporeactivity to contractile agents observed in CSE$^{-/-}$ mouse arteries, indicates a key role for cIMP. The role played by cIMP has been demonstrated by using cIMP butyrate (cell-permeable stable analogue of cIMP) that elicits a further increase in the tension on the background of phenylephrine stable tone within nanomolar concentrations, similarly to NaHS and does not exert any contractile action per se on basal tone. To further gain insight on a possible direct effect

FIGURE 10 Inosine 3′,5′-cyclic monophosphate (cIMP) butyrate causes an increase in tension in phenylephrine (PE)-contracted mouse aortic rings. (a) Chemical structure of cIMP butyrate, (b) representative trace of concentration–response curves induced by cIMP butyrate (0.1 nM to 1 μM) on basal tone, (c) cIMP butyrate (0.1 nM to 1 μM, $n = 8$ mice) causes an increase in contraction on PE stable tone ($n = 10$ mice). Values shown are means ± SEM and expressed as δ increase in tension over PE contraction (dyne/mg tissue). *$P < 0.05$ significantly different as indicated; two-way ANOVA with Bonferroni's post hoc test
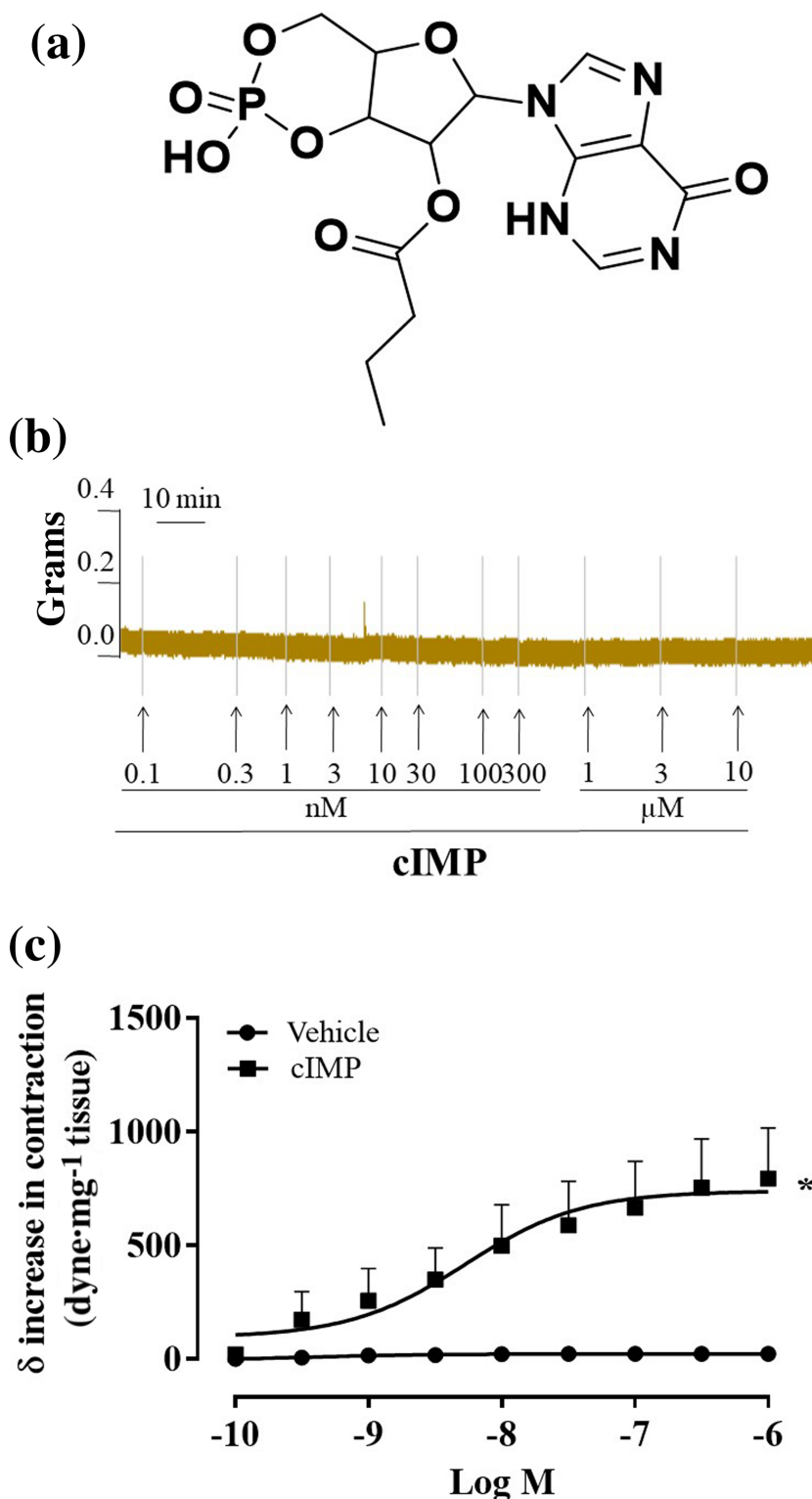
of hydrogen sulfide on sGC has been investigated in a cell-free assay. NaHS does not favour basal or NO-stimulated cIMP synthesis by recombinant sGC. The lack of a direct positive modulation of recombinant sGC by H₂S in vessel function was confirmed by the finding that NaHS-induced vasorelaxation in endothelium-intact aorta tissue but this was not modified by selective sGC inhibitors (Brancaleone et al., 2008; Zhao & Wang, 2002).

Having ruled out a possible direct effect on sGC activity, we concentrated on the most abundantly expressed PDE isoforms in vasculature, PDE5 and PDE4D that degrade cGMP and cAMP, respectively (Francis et al., 2011). PDE activation is tightly regulated by the binding of the cyclic nucleotide and by post-translational mechanism, that is phosphorylation. It is well accepted that PDE phosphorylation constitutes a post-translational event leading to an increase in PDE activity

(Francis et al., 2011). For this reason, pPDE/PDE ratio is considered as an indirect index of PDE activity. Western blot analysis demonstrates that nanomolar concentration of NaHS promotes, within vessels, the rapid phosphorylation of PDE4A and PDE5 which in turn leads to enhanced degradation of both cAMP and cGMP but not cIMP. Therefore, the reduced availability of both cAMP and cGMP uncovers cIMP signalling which leads to a contractile effect. We have previously demonstrated that H$_2$S at micromolar concentration acts as a nonselective inhibitor of PDE activity, inducing an increase of both cAMP and cGMP levels and thereby leading to vasorelaxation (Bucci et al., 2010). This apparent contradiction can be reconciled considering the hydrogen sulfide concentration. Indeed, H$_2$S-induced vasorelaxation occurs within a range of concentrations of 30–100 μM, whilst the H$_2$S-induced contraction appears within the nanomolar range (10 nM to 3 μM). Another important aspect is the timeframe within which hydrogen sulfide-induced contraction takes place. We have shown that the reduction of both cAMP and cGMP is already significant after 5 min from NaHS incubation. These data fit well with the time needed to elicit contraction in phenylephrine precontracted rings and for PDE activation following NaHS exposure. Indeed, a significant increase of pPDE/PDE ratio appears within a timeframe of 5 min. The fact that hydrogen sulfide negatively modulates cAMP production has been already reported in rat vascular smooth muscle cells, where NaHS blunts forskolin-induced cAMP accumulation (Lim et al., 2008). However, direct positive modulation of H$_2$S on both adenylyl cyclase (AC) and sGC activity cannot be excluded. In particular, several studies suggest that hydrogen sulfide could activate AC when the enzyme is in resting condition (Hu et al., 2008; Kimura, 2000; Nishikawa et al., 2013). However, if and how hydrogen sulfide could directly activate AC remains unclear.

In conclusion, CSE-derived H$_2$S contributes to the vessel homeostasis also by modulating the contractile tone, besides its vasorelaxant action. The endothelium plays an obligatory role that involves both the NO and hydrogen sulfide pathways. This interaction is dynamically regulated through the action of hydrogen sulfide on the phosphodiesterases modulating the ratio among cIMP, cGMP and cAMP defining a previously undescribed key role for cIMP in the fine regulation of vascular homeostasis.

AUTHOR CONTRIBUTIONS

E.M. and V.V. conducted experiments, analysed data and wrote the manuscript; V.B. conducted experiments, analysed data and revised the manuscript; D.V. and O.L.M. conducted experiments; E.M., I.S. and Y.K. conducted experiments for guanyly cyclase activity and analysed the data; M.C.M. and E.M. conducted experiments for nucleotides determination and analysed the data; F.F. and G.C. designed and performed cIMP butyrate synthesis; A.P. designed sGC experiments and cIMP studies and revised the manuscript; G.C. conceived and designed the study, revised the manuscript and gave final approve; R.S. analysed data and revised the manuscript; R.d.V.B. and M.B. conceived and designed the study and wrote the manuscript.

CONFLICT OF INTEREST

The authors declare no conflict of interest.

DECLARATION OF TRANSPARENCY AND SCIENTIFIC RIGOUR

This Declaration acknowledges that this paper adheres to the principles for transparent reporting and scientific rigour of preclinical research as stated in the *British journal of Pharmacology* guidelines for Design & Analysis, Immunoblotting and Immunochemistry and Animal Experimentation, and as recommended by funding agencies, publishers and other organisations engaged with supporting research.

DATA AVAILABILITY STATEMENT

The data that support the findings of this study are available from the corresponding author upon reasonable request. Some data may not be made available because of privacy or ethical restrictions.

ORCID

Emma Mitidieri https://orcid.org/0000-0003-4372-9611
Valentina Vellecco https://orcid.org/0000-0002-5674-9112
Vincenzo Brancaleone https://orcid.org/0000-0002-0063-659X
Elva Morretta https://orcid.org/0000-0002-7244-0297
Raffaella Sorrentino https://orcid.org/0000-0002-0284-5424
Roberta d'Emmanuele di Villa Bianca https://orcid.org/0000-0003-0992-6400
Mariarosaria Bucci https://orcid.org/0000-0001-5502-4315

REFERENCES

Alexander, S. P. H., Christopoulos, A., Davenport, A. P., Kelly, E., Mathie, A., Peters, J. A., Yao, C., Veale, E. L., Armstrong, J. F., Faccenda, E., Harding, S. D., Pawson, A. J., Sharman, J. L., Southan, C., Davies, J. A., Abbracchio, M. P., Alexander, W., Al-hosaini, K., Bäck, M., … CGTP Collaborators. (2019). The Concise Guide to PHARMACOLOGY 2019/20: G protein-coupled receptors. *British Journal of Pharmacology*, *176*(Suppl 1), S21–S141. https://doi.org/10.1111/bph.14748

Alexander, S. P. H., Roberts, R. E., Broughton, B. R. S., Sobey, C. G., George, C. H., Stanford, S. C., Cirino, G., Docherty, J. R., Giembycz, M. A., Hoyer, D., Insel, P. A., Izzo, A. A., Ji, Y., MacEwan, D. J., Mangum, J., Wonnacott, S., & Ahluwalia, A. (2018). Goals and practicalities of immunoblotting and immunohistochemistry: A guide for submission to the British Journal of pharmacology. *British Journal of Pharmacology*, *175*(3), 407–411. https://doi.org/10.1111/bph.14112

Beste, K. Y., Burhenne, H., Kaever, V., Stasch, J. P., & Seifert, R. (2012). Nucleotidyl cyclase activity of soluble guanylyl cyclase α$_1$β$_1$. *Biochemistry*, *51*(1), 194–204. https://doi.org/10.1021/bi201259y

Brancaleone, V., Roviezzo, F., Vellecco, V., De Gruttola, L., Bucci, M., & Cirino, G. (2008). Biosynthesis of H$_2$S is impaired in non-obese diabetic (NOD) mice. *British Journal of Pharmacology*, *155*(5), 673–680. https://doi.org/10.1038/bjp.2008.296

Brancaleone, V., Vellecco, V., Matassa, D. S., d'Emmanuele di Villa Bianca, R., Sorrentino, R., Ianaro, A., Bucci, M., Esposito, F., & Cirino, G. (2015). Crucial role of androgen receptor in vascular H_2S biosynthesis induced by testosterone. *British Journal of Pharmacology*, *172*(6), 1505–1515. https://doi.org/10.1111/bph.12740

Bucci, M., Papapetropoulos, A., Vellecco, V., Zhou, Z., Pyriochou, A., Roussos, C., Roviezzo, F., Brancaleone, V., & Cirino, G. (2010). Hydrogen sulfide is an endogenous inhibitor of phosphodiesterase activity. *Arteriosclerosis, Thrombosis, and Vascular Biology*, *30*(10), 1998–2004. https://doi.org/10.1161/ATVBAHA.110.209783

Chauhan, S., Jelen, F., Sharina, I., & Martin, E. (2012). The G-protein regulator LGN modulates the activity of the NO receptor soluble guanylate cyclase. *The Biochemical Journal*, *446*(3), 445–453. https://doi.org/10.1042/BJ20111882

Chen, Z., Zhang, X., Ying, L., Dou, D., Li, Y., Bai, Y., Liu, J., Liu, L., Feng, H., Yu, X., Leung, S. W. S., Vanhoutte, P. M., & Gao, Y. (2014). cIMP synthesized by sGC as a mediator of hypoxic contraction of coronary arteries. *American Journal of Physiology. Heart and Circulatory Physiology*, *307*(3), H328–H336. https://doi.org/10.1152/ajpheart.00132.2014

Cirino, G., Vellecco, V., & Bucci, M. (2017). Nitric oxide and hydrogen sulfide: The gasotransmitter paradigm of the vascular system. *British Journal of Pharmacology*, *174*(22), 4021–4031. https://doi.org/10.1111/bph.13815

Coletta, C., Papapetropoulos, A., Erdelyi, K., Olah, G., Modis, K., Panopoulos, P., Asimakopoulou, A., Gero, D., Sharina, I., Martin, E., & Szabo, C. (2012). Hydrogen sulfide and nitric oxide are mutually dependent in the regulation of angiogenesis and endothelium-dependent vasorelaxation. *Proceedings of the National Academy of Sciences of the United States of America*, *109*(23), 9161–9166. https://doi.org/10.1073/pnas.1202916109

Curtis, M. J., Alexander, S., Cirino, G., Docherty, J. R., George, C. H., Giembycz, M. A., Hoyer, D., Insel, P. A., Izzo, A. A., Ji, Y., MacEwan, D. J., Sobey, C. G., Stanford, S. C., Teixeira, M. M., Wonnacott, S., & Ahluwalia, A. (2018). Experimental design and analysis and their reporting II: Updated and simplified guidance for authors and peer reviewers. *British Journal of Pharmacology*, *175*(7), 987–993. https://doi.org/10.1111/bph.14153

Davenport, A. P., Hyndman, K. A., Dhaun, N., Southan, C., Kohan, D. E., Pollock, J. S., Pollock, D. M., Webb, D. J., & Maguire, J. J. (2016). Endothelin. *Pharmacological Reviews*, *68*(2), 357–418. https://doi.org/10.1124/pr.115.011833

d'Emmanuele di Villa Bianca, R., Sorrentino, R., Coletta, C., Mitidieri, E., Rossi, A., Vellecco, V., Pinto, A., Cirino, G., & Sorrentino, R. (2011). Hydrogen sulfide-induced dual vascular effect involves arachidonic acid cascade in rat mesenteric arterial bed. *The Journal of Pharmacology and Experimental Therapeutics*, *337*(1), 59–64. https://doi.org/10.1124/jpet.110.176016

Detremmerie, C. M., Chen, Z., Li, Z., Alkharfy, K. M., Leung, S. W., Xu, A., Gao, Y., & Vanhoutte, P. M. (2016). Endothelium-dependent contractions of isolated arteries to thymoquinone require biased activity of soluble guanylyl cyclase with subsequent cyclic IMP production. *The Journal of Pharmacology and Experimental Therapeutics*, *358*(3), 558–568. https://doi.org/10.1124/jpet.116.234153

Dhaun, N., & Webb, D. J. (2019). Endothelins in cardiovascular biology and therapeutics. *Nature Reviews. Cardiology*, *16*(8), 491–502. https://doi.org/10.1038/s41569-019-0176-3

di d'Emmanuele di Villa Bianca, R., Coletta, C., Mitidieri, E., De Dominicis, G., Rossi, A., Sautebin, L., Cirino, G., Bucci, M., & Sorrentino, R. (2010). Hydrogen sulphide induces mouse paw oedema through activation of phospholipase A_2. *British Journal of Pharmacology*, *161*(8), 1835–1842.

Francis, S. H., Houslay, M. D., & Conti, M. (2011). Phosphodiesterase inhibitors: Factors that influence potency, selectivity, and action. *Handbook of Experimental Pharmacology*, (204), 47–84.

Gao, Y., Chen, Z., Leung, S. W., & Vanhoutte, P. M. (2015). Hypoxic vasospasm mediated by cIMP: When soluble guanylyl cyclase turns bad. *Journal of Cardiovascular Pharmacology*, *65*(6), 545–548. https://doi.org/10.1097/FJC.0000000000000167

Hu, H., Shi, Y., Chen, Q., Yang, W., Zhou, H., Chen, L., Tang, Y., & Zheng, Y. (2008). Endogenous hydrogen sulfide is involved in regulation of respiration in medullary slice of neonatal rats. *Neuroscience*, *156*(4), 1074–1082. https://doi.org/10.1016/j.neuroscience.2008.08.025

Jia, L., & Furchgott, R. F. (1993). Inhibition by sulfhydryl compounds of vascular relaxation induced by nitric oxide and endothelium-derived relaxing factor. *The Journal of Pharmacology and Experimental Therapeutics*, *267*(1), 371–378.

Kilkenny, C., Browne, W., Cuthill, I. C., Emerson, M., & Altman, D. G. (2010). Animal research: Reporting in vivo experiments: The ARRIVE guidelines. *British Journal of Pharmacology*, *160*(7), 1577–1579. https://doi.org/10.1111/j.1476-5381.2010.00872.x

Kimura, H. (2000). Hydrogen sulfide induces cyclic AMP and modulates the NMDA receptor. *Biochemical and Biophysical Research Communications*, *267*(1), 129–133. https://doi.org/10.1006/bbrc.1999.1915

Kubo, S., Kajiwara, M., & Kawabata, A. (2007). Dual modulation of the tension of isolated gastric artery and gastric mucosal circulation by hydrogen sulfide in rats. *Inflammopharmacology*, *15*(6), 288–292. https://doi.org/10.1007/s10787-007-1590-4

Leung, S. W. S., Gao, Y., & Vanhoutte, P. M. (2017). 3′,5′-cIMP as potential second messenger in the vascular wall. *Handbook of Experimental Pharmacology*, *238*, 209–228. https://doi.org/10.1007/164_2015_39

Lilley, E., Stanford, S. C., Kendall, D. E., Alexander, S. P. H., Cirino, G., Docherty, J. R., George, C. H., Insel, P. A., Izzo, A. A., Ji, Y., Panettieri, R. A., Sobey, C. G., Stefanska, B., Stephens, G., Teixeira, M., & Ahluwalia, A. (2020). ARRIVE 2.0 and the British Journal of pharmacology: Updated guidance for 2020. *British Journal of Pharmacology*, *177*(16), 3611–3616. https://doi.org/10.1111/bph.15178

Lim, J. J., Liu, Y. H., Khin, E. S., & Bian, J. S. (2008). Vasoconstrictive effect of hydrogen sulfide involves downregulation of cAMP in vascular smooth muscle cells. *American Journal of Physiology. Cell Physiology*, *295*(5), C1261–C1270. https://doi.org/10.1152/ajpcell.00195.2008

Liu, Y. H., Yan, C. D., & Bian, J. S. (2011). Hydrogen sulfide: A novel signaling molecule in the vascular system. *Journal of Cardiovascular Pharmacology*, *58*(6), 560–569. https://doi.org/10.1097/FJC.0b013e31820eb7a1

Maguire, J. J., & Davenport, A. P. (1999). Endothelin receptor expression and pharmacology in human saphenous vein graft. *British Journal of Pharmacology*, *126*(2), 443–450. https://doi.org/10.1038/sj.bjp.0702326

Mazzuca, M. Q., & Khalil, R. A. (2012). Vascular endothelin receptor type B: Structure, function and dysregulation in vascular disease. *Biochemical Pharmacology*, *84*(2), 147–162. https://doi.org/10.1016/j.bcp.2012.03.020

Mergia, E., Friebe, A., Dangel, O., Russwurm, M., & Koesling, D. (2006). Spare guanylyl cyclase NO receptors ensure high NO sensitivity in the vascular system. *The Journal of Clinical Investigation*, *116*(6), 1731–1737. https://doi.org/10.1172/JCI27657

Mitidieri, E., Tramontano, T., Gurgone, D., Citi, V., Calderone, V., Brancaleone, V., Katsouda, A., Nagahara, N., Papapetropoulos, A., Cirino, G., d'Emmanuele di Villa Bianca, R., & Sorrentino, R. (2018). Mercaptopyruvate acts as endogenous vasodilator independently of 3-mercaptopyruvate sulfurtransferase activity. *Nitric Oxide*, *75*, 53–59. https://doi.org/10.1016/j.niox.2018.02.003

Miyauchi, T., & Masaki, T. (1999). Pathophysiology of endothelin in the cardiovascular system. *Annual Review of Physiology*, *61*, 391–415. https://doi.org/10.1146/annurev.physiol.61.1.391

Nishikawa, H., Hayashi, H., Kubo, S., Tsubota-Matsunami, M., Sekiguchi, F., & Kawabata, A. (2013). Inhibition by hydrogen sulfide of rabbit platelet aggregation and calcium mobilization. *Biological &*

Pharmaceutical Bulletin, 36(8), 1278–1282. https://doi.org/10.1248/bpb.b13-00018

Percie du Sert, N., Hurst, V., Ahluwalia, A., Alam, S., Avey, M. T., Baker, M., Browne, W. J., Clark, A., Cuthill, I. C., Dirnagl, U., Emerson, M., Garner, P., Holgate, S. T., Howells, D. W., Karp, N. A., Lazic, S. E., Lidster, K., MacCallum, C. J., Macleod, M., … Würbel, H. (2020). The ARRIVE guidelines 2.0: updated guidelines for reporting animal research. *PLoS Biology*, 18(7), e3000410. https://doi.org/10.1371/journal.pbio.3000410

Posternak, T., & Weimann, G. (1974). The preparation of acylated derivatives of cyclic nucleotides. *Methods in Enzymology*, 38, 399–409. https://doi.org/10.1016/0076-6879(74)38057-3

Reinecke, D., Burhenne, H., Sandner, P., Kaever, V., & Seifert, R. (2011). Human cyclic nucleotide phosphodiesterases possess a much broader substrate-specificity than previously appreciated. *FEBS Letters*, 585(20), 3259–3262. https://doi.org/10.1016/j.febslet.2011.09.004

Severino, B., Corvino, A., Fiorino, F., Luciano, P., Frecentese, F., Magli, E., Saccone, I., di Vaio, P., Citi, V., Calderone, V., Servillo, L., Casale, R., Cirino, G., Vellecco, V., Bucci, M., Perissutti, E., Santagada, V., & Caliendo, G. (2018). 1,2,4-Thiadiazolidin-3,5-diones as novel hydrogen sulfide donors. *European Journal of Medicinal Chemistry*, 143, 1677–1686. https://doi.org/10.1016/j.ejmech.2017.10.068

Sharina, I. G., Sobolevsky, M., Papakyriakou, A., Rukoyatkina, N., Spyroulias, G. A., Gambaryan, S., & Martin, E. (2015). The fibrate gemfibrozil is a NO- and haem-independent activator of soluble guanylyl cyclase: In vitro studies. *British Journal of Pharmacology*, 172(9), 2316–2329. https://doi.org/10.1111/bph.13055

Vellecco, V., Mitidieri, E., Gargiulo, A., Brancaleone, V., Matassa, D., Klein, T., Esposito, F., Cirino, G., & Bucci, M. (2016). Vascular effects of linagliptin in non-obese diabetic mice are glucose-independent and involve positive modulation of the endothelial nitric oxide synthase (eNOS)/caveolin-1 (CAV-1) pathway. *Diabetes, Obesity & Metabolism*, 18(12), 1236–1243. https://doi.org/10.1111/dom.12750

Webb, G. D., Lim, L. H., Oh, V. M., Yeo, S. B., Cheong, Y. P., Ali, M. Y., El Oakley, R., Lee, C. N., Wong, P. S., Caleb, M. G., & Salto-Tellez, M. (2008). Contractile and vasorelaxant effects of hydrogen sulfide and its biosynthesis in the human internal mammary artery. *The Journal of Pharmacology and Experimental Therapeutics*, 324(2), 876–882. https://doi.org/10.1124/jpet.107.133538

White, A. A. (1974). Separation and purification of cyclic nucleotides by alumina column chromatography. *Methods in Enzymology*, 38, 41–46. https://doi.org/10.1016/0076-6879(74)38009-3

Yu, W., Jin, H., Tang, C., Du, J., & Zhang, Z. (2018). Sulfur-containing gaseous signal molecules, ion channels and cardiovascular diseases. *British Journal of Pharmacology*, 175(8), 1114–1125. https://doi.org/10.1111/bph.13829

Zhao, W., & Wang, R. (2002). H_2S-induced vasorelaxation and underlying cellular and molecular mechanisms. *American Journal of Physiology. Heart and Circulatory Physiology*, 283(2), H474–H480. https://doi.org/10.1152/ajpheart.00013.2002

Zhao, W., Zhang, J., Lu, Y., & Wang, R. (2001). The vasorelaxant effect of H_2S as a novel endogenous gaseous K_{ATP} channel opener. *The EMBO Journal*, 20(21), 6008–6016. https://doi.org/10.1093/emboj/20.21.6008

Zuidema, M. Y., Yang, Y., Wang, M., Kalogeris, T., Liu, Y., Meininger, C. J., Hill, M. A., Davis, M. J., & Korthuis, R. J. (2010). Antecedent hydrogen sulfide elicits an anti-inflammatory phenotype in postischemic murine small intestine: Role of BK channels. *American Journal of Physiology. Heart and Circulatory Physiology*, 299(5), H1554–H1567. https://doi.org/10.1152/ajpheart.01229.2009

SUPPORTING INFORMATION

Additional supporting information may be found online in the Supporting Information section at the end of this article.